

T.R.
VAN YUZUNCU YIL UNIVERSITY
INSTITUTE OF NATURAL AND APPLIED SCIENCES
DEPARTMENT OF PHYSICS

**FABRICATION OF ORGANIC-BASED PHOTODIODE AND
DETERMINATION OF ITS PARAMETERS FOR THE OPTOELECTRONIC
APPLICATIONS**

M. Sc. THESIS

PREPARED BY: Othman Haji MAHMOOD
SUPERVISOR: Assoc. Prof. Dr. Arife GENÇER İMER

VAN-2020

T.R.
VAN YUZUNCU YIL UNIVERSITY
INSTITUTE OF NATURAL AND APPLIED SCIENCES
DEPARTMENT OF PHYSICS

**FABRICATION OF ORGANIC-BASED PHOTODIODE AND
DETERMINATION OF ITS PARAMETERS FOR THE OPTOELECTRONIC
APPLICATIONS**

M. Sc. THESIS

PREPARED BY: Othman Haji MAHMOOD

VAN-2020

ACCEPTANCE AND APPROVAL PAGE

This thesis entitled “**DETERMINATION OF OXIDATIVE STRESS LEVELS AND SOME ANTIOXIDANT ACTIVITIES IN ACUTE AND CHRONIC RENAL FAILURE PATIENTS**” and prepared by Seerwan Hamad Ameen Sulaiman under consultation of Prof. Dr. Halit DEMİR in Department of Chemistry, on date of 27/12/2019 it has been successful with a unanimous vote by the following jury and it has been recognized as a Master’s Thesis, in accordance with Postgraduate Education and training regulation with the relevant provisions.

Supervisor: Prof. Dr. Halit DEMİR

Signature:

Member: Prof. Dr. Suat EKİN

Signature:

Member: Assist. Prof. Dr. Fikret TÜRKAN

Signature:

The Board of Directors of the Institute of Science:/...../..... date and is approved by decision No.....

Signature

.....

Director of the Institute

THESIS STATEMENT

All information presented in the thesis obtained in the frame of ethical behavior and academic rules. In addition all kinds of information that does not belong to me have been cited appropriately in the thesis prepared by the thesis writing rules.



Signature

Othman Haji MAHMOOD

ABSTRACT

FABRICATION OF ORGANIC-BASED PHOTODIODE AND DETERMINATION OF ITS PARAMETERS FOR THE OPTOELECTRONIC APPLICATIONS

MAHMOOD, Othman Haji
M. Sc. Thesis, Department of Physics
SUPERVISOR: Assoc. Prof. Dr. Arife GENÇER İMER
January, 2020, 54 Pages

In this thesis, the organic based heterojunction devices were fabricated by depositing Brilliant Blue (BB) on n-Si wafer via spin coating method and evaporating Cu metal on the film with thermal evaporation technique. Electrical and photoelectrical property of fabricated devices have been investigated. Current-voltage measurements for Cu/n-Si/Au and Cu/BB/n-Si/Au were performed in the dark and at room temperature. The main electrical parameters of devices were determined using experimental and theoretical methods such as thermionic emission theory, Cheung and modified Norde functions, and obtained results were compared each other. The results show that inserting organic interlayer cause to enhance the electrical properties of the prepared devices such as better rectification behavior, higher barrier height and lower series resistance. Additionally, the frequency dependent capacitance-voltage measurement was carried out at room temperature for devices. It was noticed that the device cannot flow A.C signals at high frequencies, thus exhibit low capacitive property. Furthermore, the current-voltage measurements were carried out under various light illuminations in the range between 30-100 mW/cm². The obtained results show that reverse bias photocurrent is strongly dependent on incident illumination power. The device also represents a high responsivity for incident light intensities. In addition, it was recognized that the device is capable to detect small amount of light intensity at low reverse voltages.

Keywords: Barrier height, MS contact, Organic materials, Photosensing, Photodiode.



ÖZET

OPTOELEKTRONİK UYGULAMALAR İÇİN ORGANİK BİLEŞENLİ FOTODİYOTUN ÜRETİMİ VE PARAMETRELERİNİN BELİRLENMESİ

MAHMOOD, Othman Haji
Yüksek Lisans Tezi, Fizik Anabilim Dalı
Tez Danışmanı: Doç. Dr. Arife GENÇER İMER
Ocak, 2020, 54 Sayfa

Bu tez çalışmasında, n-Si alttaş üzerine dönel kaplama metoduyla parlak mavi (BB) film kaplandı ve bu film üzerine bakır (Cu) üst kontaklar termal buharlaştırma tekniği ile oluşturularak organik bileşenli heteroeklem aygıt üretildi. Fabrikasyonu yapılan cihazların elektriksel ve fotoelektriksel özellikleri araştırıldı. Üretilen Cu / n-Si / Au ve Cu / BB / n-Si / Au aygıtların akım gerilim ölçümleri karanlıkta ve oda sıcaklığında gerçekleştirildi. Aygıtın temel elektriksel parametreleri, termiyonik emisyon teorisi, Cheung ve modifiye Norde fonksiyonları kullanılarak belirlendi. Farklı yöntemlerden hesaplanan elektriksel parametre değerleri karşılaştırıldı. Elde edilen sonuçlar, organik ara tabakanın arayüzey olarak kullanıldığı aygıtın daha iyi doğrultma davranışı, daha yüksek engel yüksekliği ve daha düşük seri direnç gibi elektriksel parametrelerin iyileşmesine sebep olduğu tespit edildi. Ayrıca, her iki aygıtın frekansa bağlı kapasitans gerilim ölçümü oda sıcaklığında gerçekleştirildi. Yüksek frekanslarda cihazın A.C sinyallerini takip edemediği ve dolayısıyla düşük kapasitif özelliğe sahip olduğu gösterildi. Ayrıca, akım-gerilim ölçümleri 30-100 mW/cm² aralığında değişen farklı aydınlatmalar altında gerçekleştirildi. Ters beslemde foto akımın gelen ışığın aydınlatma gününe büyük ölçüde bağlı olduğu rapor edildi. Ayrıca, aygıtın ışık duyarlılığının gelen ışık şiddeti ile ilişkili olduğu tespit edildi. Deneysel sonuçlara göre, cihazın düşük ters beslem değerinde bile ışık duyarlılığının olduğu ve optoelektronik teknolojisinde fotodiyot olarak kullanılabilirliği gösterildi.

Anahtar kelimeler: Engel yüksekliği, Fotodiyot, Işık duyarlılığı, MS eklem, Organik arayüzey.



ACKNOWLEDGEMENT

In the name of Allah, the Most Gracious and the Most Merciful.

All praises to Allah and His blessing for the completion of this thesis. I thank God for all the opportunities, trials and strength that have been showered on me to finish writing the thesis.

First and foremost, I would like to sincerely thank my supervisor Assoc. Prof. .Dr. Arife Gençer Imer for her guidance, understanding, patience and most importantly, she has provided positive encouragement and a warm spirit to finish this thesis. It has been a great pleasure and honour to have her as my supervisor.

My deepest gratitude goes to all of my family members. It would not be possible to write this thesis without the support from them. I would like to thank my dearest father Haji Mahmood, my mother Zerine, my lover wife Hawzhin, my dear son Wanyar and my little girl Nwa.

I would like to pay my special regards to Assoc. Prof. Dr. Murat AYCIBİN and Mr.Ahmed Abdulrahman for their efforts and helping me in language proofing for my thesis. Also I offer my thanks to Dr. Abdulkadir Korkut for his helping to me in the laboratory when I performed experiments May God shower the above cited personalities with success and honour in their life.

January 2020

OTHMAN HAJI MAHMMO



TABLE OF CONTENTS

	Pages
ABSTRACT	i
ÖZET	iii
ACKNOWLEDGEMENT	v
TABLE OF CONTENTS	vii
LIST OF TABLES	ix
LIST OF FIGURES	xi
SYMBOLS AND ABBREVIATIONS	xiii
1. INTRODUCTION	1
2. LITERATURE SUMMARY	3
3. THEORETICAL BACKGROUND	7
3.1. Semiconductors	7
3.1.1. Intrinsic semiconductors	7
3.1.2. Extrinsic semiconductors	9
3.2. Organic Materials	10
3.3. Metal-Semiconductor Heterojunctions.....	11
3.3.1. Rectifier contact	11
3.4. Electrical Parameters of Metal-Semiconductor Contact	13
3.4.1. Ideality factor	13
3.4.2. Series resistance	14
3.4.3. Barrier height.....	14
3.5. Photo-Sensing Parameters of Photodetector	15
3.5.1. Responsivity	16
3.5.2. Detectivity	16
3.5.3. Linear dynamic range.....	17
4. EXPERIMENTAL METHOD	19
4.1. Silicon Wafer Cleaning	19
4.2. Formation of Ohmic Contact.....	19

	Pages
4.3. Deposition of Organic Layer Thin Film.....	21
4.4. Formation of Rectifier Contact.....	22
4.5. Analyzing Method.....	22
5. RESULTS AND DISCUSSION.....	25
5.1 Current-Voltage Measurement For Diodes Under Dark	25
5.2 Capacitance -Voltage Measurement.....	30
5.3 Photoelectrical Properties of Cu/BB/N-Si/Au Photodiode	34
6. CONCLUSION	41
REFERENCES	43
EXTENDED TURKISH SUMMARY (GENİŞLETİLMİŞ TÜRKÇE ÖZET).....	47
CURRICULUM VITAE.....	53

LIST OF TABLES

Table	Pages
Table 4.1 RCA cleaning steps	20
Table 5.1 Electrical parameters for Cu/n-Si/Au and Cu/BB/n-Si/Au diodes determined from I-V measurements	30
Table 5.2 Electrical parameters for Cu/n-Si/Au and Cu/BB/n-Si/Au diodes determined from C-V measurements.	32





LIST OF FIGURES

Figures	Pages
Figure 1.1 Molecular structure of brilliant blue	2
Figure 3.1 Energy band diagram for metal and n-type semiconductor if $\phi_m > \phi_s$ (a) before contact (b) after contact at thermal equilibrium and produce rectifier contact.....	11
Figure 3.2 Energy band diagram for metal–(n-type) semiconductor junction with interfacial layer	15
Figure 4.1 Thermal evaporaton machine used to evaporate metal.....	21
Figure 4.2 Furnace used to thermal annealing.....	21
Figure 4.3 Spin coater used to deposite organic thin film layer.....	22
Figure 4.4 Schematic diagram of Cu/BB/n-Si/Au.....	23
Figure 4.5 Keithley 2400 Sourcemeter.....	23
Figure 4.6 HP agilent 4294A impedance analyzer.....	24
Figure 5.1 Semi-logarithmic I-V plots for Cu/BB/n-Si/Au and Cu/n-Si/Au diodes in dark.....	26
Figure 5.2 $dV/d\ln I$ versus I for Cu/n-Si/Au and Cu/BB/n-Si/Au diodes.	28
Figure 5.3 $H(I)$ versus I plots for Cu/n-Si/Au and Cu/BB/n-Si/Au diodes.	28
Figure 5.4 Norde's function plots for Cu/n-Si/Au and Cu/BB/n-Si/Au diodes.	29
Figure 5.5 Capacitance - voltage measureent for Cu/n-Si/Au diode at variou frequencies	31
Figure 5.6 Capacitance - voltage measurements for Cu/BB/n-Si/Au diode at various frequencies.....	31
Figure 5.7 Reverse C^{-2} -V characteristic for Cu/n-Si/Au diode diode in room temperature and at 500 kHz.....	33
Figure 5.8 Reverse C^{-2} -V characteristic for Cu/BB/n-Si/Au diode diode in room temperature and at 500 kHz.....	33
Figure 5.9 Reverse and forward bias $\ln I$ -V plots of Cu/BB/n-Si/Au photodiode in dark and under various illuminations at room temperature.	34
Figure 5.10 The relation between $\text{Log} I_{ph}$ versus $\text{Log} P$ at various reverse biasing voltages for Cu/BB/n-Si/Au photodiode.....	35

Figures	Pages
Figure 5.11 The relation between photocurrent and incident power at various reverse biasing voltages for Cu/BB/n-Si/Au photodiode	36
Figure 5.12 Photoresponsivity as a function of reverse biasing voltages under different illuminations for Cu/BB/n-Si/Au photodiode.....	37
Figure 5.13 Represents the variation detectivity with respect reverse bias voltage for Cu/BB/n-Si/Au photodiode under various light intensities.	38
Figure 5.14 Variation of linear dynamic range with respect of reverse bias voltage.....	39



SYMBOLS AND ABBREVIATIONS

Some symbols and abbreviations used in this study are presented below, along with Descriptions.

Symbols	Description
BB	Brilliant blue
MS	Metal-semiconductor junction
MIS	Metal-insulator-semiconductor contact
p-Si	p type silicon substrate
n-Si	n type silicon substrate
Cu	Copper
Au	Gold
SiC	Silicon carbide
Al	Aluminum
QY	Quinoline yellow dye
n(T)	Number of electrons in conduction band
p(T)	Number of holes in valence band
n_i	Intrinsic carrier concentration
N_c	Effective DOS in the conduction band
N_v	Effective DOS in the valence band
E_g	Energy gap
k_B	Boltzman constant
T	Temperature
E_c	Bottom of the conduction band
E_v	Top of the valence band
e	Electron charge
V_{bi}	Built in voltage
ϕ_m	Metal work function
ϕ_s	Semiconductor work function
ϕ_{Bn}	Barrier height for n-type semiconductor

Symbols	Description
ϕ_{Bp}	Barrier height for p-type semiconductor
I_0	Saturation current
A	Effective contact area
A^*	Richardson constant
n	Ideality factor
ϕ_0	Barrier height at zero voltage
D_s	Density of states
ϵ_s	Dielectric constant of semiconductors
ϵ_i	Dielectric constant of interfacial layer
δ	Interfacial layer thickness
R	Responsivity
I_{ph}	Photocurrent
P	Illuminated power
A	Illuminated area
D^*	Specific detectivity

1. INTRODUCTION

Today, semiconductor technology is the most studied technology in the world because of whole electronic devices manufactured based on semiconductors. Generally, organic materials have a great benefit in wide range electrical and optoelectronic applications, on account of their excellent electrical, thermal and chemical properties. In the last years, many researchers have concentrated on using organic based compounds due to their advantages such as the low-cost synthesis, the easy preparation and the possibility of large area applications.

Since Walter H. Schottky fabricated a new generation of diode with high efficiency and wide range usage possibility, this diode caused attract more attention of researchers and scientist have been lead to enhance its properties. Although this kind of diode has some disadvantages like low rectifying property, inappropriate in high frequency performance, relatively high reverse/leakage current and low breakdown voltage. Scientist focused on enhancing its electrical and optoelectronic properties with many different techniques such as adding doping and inserting oxide or organic layers. Among all of techniques, inserting an organic layer is a unique way to improve electrical and optoelectrical properties of diode. Inserting an interfacial organic layer between metal and semiconductor materials may to create another different interface space of charges with bias; This is because of produce an extra electrical field in the interfacial layer. This extra field leads to enhance the electrical parameters of diodes (Yaşar et al., 2018). Adding an organic layer can be develop the performance of devices because it causes to minimize surface states, leakage current, series resistance, and surface damage. Also, an organic interfacial layer has advantage to limit localized trap states in metal-semiconductor junction to accomplish high performance for these devices (Imer and Ocak, 2016).

In literature there are a lot of methods to fabricate thin films such as vacuum evaporation, ion plating, spin coating, sputtering and chemical vapor deposition. In this thesis thermal vacuum evaporation technique was used for depositing metal on n-si substrate because of its unique ability in forming a uniform and high-purity thin films with different area dots according to desired purposes. Also, spin coating has been

applied for deposit organic dye onto substrate due to its properties such as cheap, easy processing, obtain the uniform thin film, capable to deposit multi-layer films and fast drying time due to high spin speed.

Brilliant Blue FCF, with chemical formula $C_{37}H_{34}N_2Na_2O_9S_3$ is an organic compound classified as a blue triarylmethane dye, (from Sigma-Aldrich). It is a good candidate to be used as organic interfacial between metal and semiconductor for formation purpose of thin film in this study owing to its richness in π – electrons, localized trap states, high enough dielectric constant. It has been expected to produce dipole in interface so this dipole play an important role in modification electrical and optoelectrical device. Molecular structure of brilliant blue is shown in Figure 1.1. In this thesis, it was purpose to fabricate organic Schottky diode and examine possibility using in photo sensing application. For this aim, Cu/n-Si/Au diodes were prepared. Au back contact evaporated on the n-Si substrate via physical thermal evaporation method. For obtaining ohmic contact, It was annealed in 570 °C for 3 min in N_2 atmosphere.

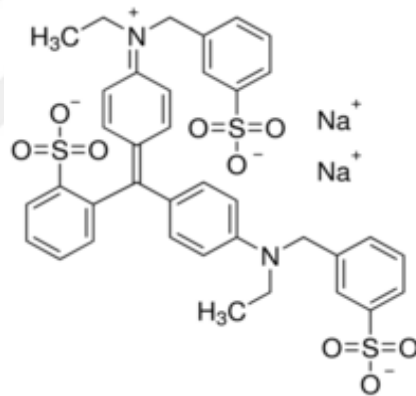


Figure 1. 1 Molecular structure of brilliant blue.

After, brilliant blue was deposited on the substrate via spin coating technique. Finally, Cu top contact was evaporated on the substrate for forming dots with inserting mask. For determining electrical and optoelectrical parameters of the diode, current-voltage characteristic was performed under dark and different solar simulator intensities. Electrical and optoelectrical parameters were calculated. Additionally, frequency dependent capacitance-voltage measurement was carried out to determine some electrical parameters such as barrier height, Fermi level and donor concentration.

2. LITERATURE REVIEW

The first electronic device was created by Joseph Henry in 1835. It was just a remote switch controlled by electricity (H.bassler, 2011). In 1874, Braun made up first semiconductor device. He reported that this device deviated from linearity (Ohm's law) in positive voltage ranges. J. C. Bose earned US patent for the metal-semiconductor (MS) diode in 1904. G.W. Pickard was first who fabricated point-contact rectifier using silicon wafer in 1907 and took patent.

In 1907 the first paper published by G.W. Pierce (Pierce, 1907), he prepared the first metal-semiconductor contacts and used silicon carbide (SiC) as a semiconductor material. After he was winded two different types of metal wire around the two ends of silicon carbide (SiC) sample. Then, he performed Current-Voltage measurement under different temperatures and pressures for the sample, he noticed that, in positive voltages region, current increase exponentially with voltage. While in negative voltages, the most of current is blocked except a little amount of leakage current passing through the device.

The essential significant investigation on rectifying properties of MS contact was performed by Schottky, Stormer and Waibel in 1931. They reported that the rectification occurred in contact due to potential drop across whole contact as current flow in it. After its investigations, Wilson built up the hypothesis of quantum mechanical tunneling and clarified the rectification by using reverse polarity (Obaid, 2015). Schottky was first scientist who could define majority carrier work functions, and called it the barrier height. According to Schottky findings (Schottky, 1939), the energy distance between the Fermi level and the edge of the respective majority band is called barrier height. In 1939 N.F. Mott proposed theory (Mott, 1939) and he explained there is a potential barrier which electrons penetrate the junction by the tunnel effect at metal semiconductor interface. This theory means the device exhibit rectification property in the opposite direction. Also, he explained the nature of the potential barrier, according to his theory, electrons require to thermally exciting to overcome the potential barrier. Even Schottky and Mott performed the similar work independently, their results are in

good agreement with each other. Today, their work is known as the Schottky Mott theory. In summary, both Schottky and Mott defined the barrier height at the metal-semiconductor interface as the difference between the work function of the metal and electron affinity of the MS contact.

The influence of high series resistance on forward bias Current-Voltage (I-V) characteristic was studied by H. Norde in 1979 for non-ideal contact (Norde, 1979). S.K. Cheung and N.W. Cheung introduced the new method to extract electrical Schottky diode parameters from forward I-V characteristic for ideal and non-ideal devices (Cheung and Cheung, 1986) such as barrier height, ideality factor, series resistance. According to their report, the results obtained from Cheung methods, and experimentally results determined from I-V characteristics are in a good agreement with each other.

The first metal-insulator-semiconductor (MIS) contact based on organic materials was fabricated by F. Ebisawa et.al. in 1982. They prepared Al/polysiloxane/polyacetylene using photolithographic technique. They found that the conduction mechanism was same with Schottky-Richardson Mechanism (Ebisawa et al., 1983).

Tang obtained about %1 power conversion efficiency under 75 mW/cm^2 of illumination intensity, for fabricated organic solar cell based on copper phthalocyanine and perylene tetracarboxylic derivative. The charge generation was directly proportional with bias voltage (Tang, 1986).

Michael J. Sailor et al prepared organic based Schottky diode (Sailor et al., 1990). They deposited polyacetylene on both p-type and n-type on silicon substrate and concentrated to study electrical properties of the device. They concluded that it is possible to improve electrical properties of MS contact by inserting organic interlayer.

Schon et all fabricated efficient organic photovoltaic diode based on doped pentacene. They revealed that the efficiency of photovoltaic is increased by adding molecular doping. According to their report, the doped iodine or bromine has many advantages for photovoltaic properties in different ways such as increased conductivity of pentacene, the edge of optical absorption shifted to 1.4 eV, the quantum efficiency is

modified and the device performance was increased compared with undoped one (Schön et al., 2004).

Ugur et al. made up organic-inorganic heterojunction based on quinoline yellow dye (Ugur et al., 2015), They prepared Al/QY/p-Si/Al structure to investigate the electrical and optoelectrical properties. According to their report, the device with organic layer has more response to light and its optoelectrical properties were improved. Therefore, they confirmed suitability of the device for optoelectronic applications.

Fawe Guo fabricated a new kind of photodiode based on ZnO nanoparticle/polymer nanocomposite materials (Guo, 2014). According to his results, this device behaves as a diode in dark, and photoconductor under ultraviolet illumination. Furthermore, the device has appeared multiple advantageous than conventional inorganic semiconductor. Also, he brought the ZnO nanoparticles into C-TPD buffer layer of the fullerene-based photodetector. As the results successfully rise photoconductive current and decrease the noise current.

H. Kim et al. fabricated the top illuminated organic photodetector with dielectric/metal/dielectric for fabricating transparent anode, While the transparent electrode is composed of molybdenum trioxide (MoO_3)/Ag/ MoO_3 layers and zinc oxide (ZnO)/Aluminum(Al) is for the bottom cathode. They revealed that fabricated organic photodiode exhibits a high detectivity and wide range linearity (H. Kim et al., 2015).

A. Gencer Imer et al investigated possibility of controlling the photosensing property photodiode by inserting the interface layer with various thickness using sol-gel spin coating method. According to their report, the photoelectrical and photo response of device strongly affected by incident light intensity, also they confirmed photosensing feature of device is enhanced by inserting organic layer (A. Gencer Imer et al., 2016).

V. Ventalon et al studied ITO/DTS(PTTH)/Al with PC_{60}BM and PC_{70}BM as a organic material and they reported that it is a unique device for detection herbicides in water (Ventalon et al., 2016).

A.Tataroglu et al studied electrical and photoresponse properties of the photovoltaic device based on Ruthenium(II) complex as an interfacial thin layer (Tataroglu et al., 2018). Their device structure was Au/Ru(II)/n-Si photodiode. They

reported that device in reverse bias under illumination exhibit more photocurrent than under dark (i.e have photoconduction properties and high responsivity).

Kee-Tae Kim et al successfully studied organic photodiode based on organic materials using Ga-doped NiO_x as an electron-hole blocking layer between photoactive material and electrode (K. T. Kim et al., 2018). They argued that the significant decreasing in leakage current of the organic photodiode was occurred, This decreasing is reason to increase in LUMO level of the electron-hole preventing buffer layer. Also, they reported that the device has high detectivity, which equals to 1.06×10^{12} Jones.

H.Abdel-Khalek et al. prepared Al/n-Si/Cu (acac)₂/Au structure and investigated microstructural, optical and optoelectronic properties of the device using a high-resolution transmission electron microscope, spectroscopic ellipsometry, and Current-Voltage techniques. They reported that the Cu(acac)₂ polycrystalline nature exhibits high clearly resolved lattice fringes. Also, they explained that copper(II)acetylacetonate is a good absorber for UV and visible light ranges. Finally, they detailed that the device show a good light detection with intensity sensitivity in high biasing voltage (Abdel-Khalek et al. 2018).

From the literature summary, we conclude that (1) it is possible to change the electrical and photoelectrical properties of photodiode by adding an organic layer (2) the novelty of this study belongs to use brilliant blue as an organic interfacial layer in optoelectronic application because it was not investigated in the previous studies according to our searches.

In this thesis, organic based photodiode Cu/BB/n-Si/Au was fabricated with brilliant blue. Then, the electrical and optoelectrical properties of the device were investigated using different methods. The I-V measurement was performed under dark and various simulated light illuminations, and C-V characteristic was carried out under different frequencies.

3. THEORETICAL BACKGROUND

In this chapter, a brief review about semiconductors are given. After that, the physical principles of MS contact, current conduction mechanism with physical factors are explained in detail. Also, the electrical and photosensing parameters of Schottky diode are presented.

3.1. Semiconductors

According to electrical conductivity, the materials can be classified into three categories: Metal, Semiconductor and Insulator.

Semiconductors is defined as material with electrical resistivity lying in the range $10^{-2} - 10^9 \Omega\text{-m}$ (Cardona. N.D, 2010). Semiconductors can be occurred in many kinds of chemical structure with a large variety of crystalline. They can be elemental semiconductors like silicon (Si), carbon in the form of C_{60} and selenium, or binary compounds such as gallium arsenide (GaAs). Many organic materials are semiconductors like polyacetylene $(CH)_n$.

Based on doping type, semiconductors are classified into two types: intrinsic and extrinsic semiconductor.

3.1.1. Intrinsic semiconductors

The semiconductors theoretically do not contain any foreign impurities. They are known as pure or undoped semiconductors. In this type of semiconductor, electrons located in the valence band are excited to conduction by absorbing of energy. The generated electron-hole pairs are contributing in current conduction mechanism at the same time together. In intrinsic semiconductors, number of holes in the valence band continuously equivalent to the number of electrons in the conduction band. There are two important parameters to be known: i) intrinsic carrier concentration and ii) intrinsic Fermi level energy.

The intrinsic carrier concentration can be calculated via the law of mass action as follow (A.kohler, 1392):

$$n(T)p(T) = n_i^2(T) \quad (3.1)$$

where $n(T)$ is number of electrons in conduction band $p(T)$ is number of holes in valence band and n_i is the intrinsic carrier concentration

By substituting values of $n(T)$ and $p(T)$ it can be derived for final expression of n_i as follows (Gerhard Lutz, 2018):

$$n_i = \sqrt{N_c N_v} \exp\left(\frac{-E_g}{2K_B T}\right) \quad (3.2)$$

where N_c is the effective density of states in the conduction band, N_v is the effective density of states in the valence band, E_g is energy gap, K_B is Boltzman constant and T is temperature.

From Eq.(3.2), it is noticed that intrinsic carrier concentration depend on many factors such as density of states at conduction band and valence band, and inversely proportional with energy gap. It makes sense because as energy gap increase electrons require more energy to migrate from the valence band to the conduction band, also we can see intrinsic carrier concentration directly proportional with increasing temperature more bonds are broken hence number of electron-hole pairs increase. It is also shown that the number of the carriers is depend on effective density of states.

Also, it is extracted the Fermi level of these intrinsic semiconductors from non-degenerate equation of semiconductor carrier concentration as follows (H.S.Nalwa, 2001):

$$n(T) = N_c \exp\left[-(E_c - E_F)/K_B T\right] \quad (3.3)$$

$$p(T) = N_v \exp\left[-(E_F - E_v)/K_B T\right] \quad (3.4)$$

where E_c is the bottom of the conduction and E_v is the top of valence band. For intrinsic semiconductors $n(T) = p(T)$ by solving this equation, the Fermi level is expressed (Zekry, 1996):

$$E_F = \frac{E_c + E_v}{2} + \frac{1}{2} K_B T \ln\left(\frac{N_v}{N_c}\right) \quad (3.5)$$

From Eq.(3.5) the first term represents the middle of the band gap, the second part of the equation shows Fermi level depends on T and logarithmic ratio of effective density of states. Typically effective density of state in valence band is little higher than the effective density of states in conduction band. Therefore, the logarithmic ratio is a small number also $k_B T$ is equal to 0.0257 eV at room temperature (M.Rudan, 2013). So, two small numbers multiply each other is a smaller number thus almost it can be neglected second term. It means that Fermi level energy is positioned in the middle of energy gap for intrinsic semiconductors.

3.1.2. Extrinsic semiconductors

When impurities contribute significantly to the carrier concentration in the semiconductor, this type of semiconductor is known as extrinsic or doped semiconductor. The extrinsic semiconductor has their own electron concentration or hole concentration, which essentially belongs to the ratio of doping present in the semiconductor and the type of impurities (Pearsall, 2013).

According to kind of impurity, extrinsic semiconductors are classified into two categories: n-type and p-type. When impurities give extra electrons to conduction mechanism then those impurities called donor, such as phosphate, and the semiconductor is called n-type semiconductor. When impurities provide additional holes to contribute conduction mechanism, it is called acceptor impurities like Boron, it is called p-type semiconductor (Arca, 2013).

In extrinsic semiconductors, electron carriers and hole concentrations are not equal, one of them is a majority, and other is is a minority carriers. The electrical conductivity of the extrinsic semiconductors is dependent on the temperature as well as the amount of impurities. The position of Fermi level changes with the type of extrinsic semiconductors. In n-type semiconductor, it is located just in below of conduction band of semiconductor. In p-type semiconductor, it is located just above the valence band of semiconductor (Sze, 2007).

3.2. Organic Materials

Organic materials are compounds based on presence carbon, they can be found both in nature and also manufacturing produce. Sometimes, organic molecules are made up from chemical reactions. In the recent years, researchers show that using organic materials has some benefits in the electronic devices due to low cost, light weight and their flexible properties. Additionally, researchers state that may organic materials became a great factor to contribute to solving today's global issues in both environmental pollution and new energy sources (Dongge and Ma Yonghua, 2017; Schlesinger, 2017). The organic materials used for optoelectronic devices are named photo and electroactive organic materials. They exhibit some special properties such as injection of the charge carriers from electrode, photo generation, transparent charge carriers, and light absorption and emission. Usually, π -electron system describes as a material. They exhibit absorbing and emitting light in the range from ultraviolet to infrared wavelengths. In addition, they have ability for generation and transportation of charge carriers in non-linear form (Arca, 2013; Brütting, 2006).

The organic materials, which are used in electronic devices, are classified as organic semiconductors. It was reported that small molecular weight organic materials are more suitable for optoelectronic applications (Ostroverkhova, 2013). Most organic semiconductors used in device fabrication are insulator without doping. In organic semiconductors, valence and conduction energy bands are replaced by the Lowest Unoccupied Molecular Orbital (LUMO) and Highest Occupied Molecular Orbital (HOMO) levels, respectively. Because, the density of states (DOS) distribution are not similar in organic and inorganic semiconductors. Furthermore, charge transport mechanism in organic semiconductors is quite different from inorganic semiconductors. The controlling of charge transport is responsible for the modifying of all properties of any electronic devices. Thus, it can be concluded that organic semiconductors can be used to enhance the electrical performance of devices (Mori, 2016).

3.3. Metal-Semiconductor Heterojunctions

When metal and semiconductor has been brought and contacted together, they form metal-semiconductor contact. Since the first invention, metal semiconductor contact attracts scientist attentions due to own high efficiency, low power consumption and its rectifying behavior. Today, there are many properties that make it convenient for wide application and become unique over the other junction devices. Metal-semiconductor contact consists two parts, one side is ohmic contact and another side is rectifier contact.

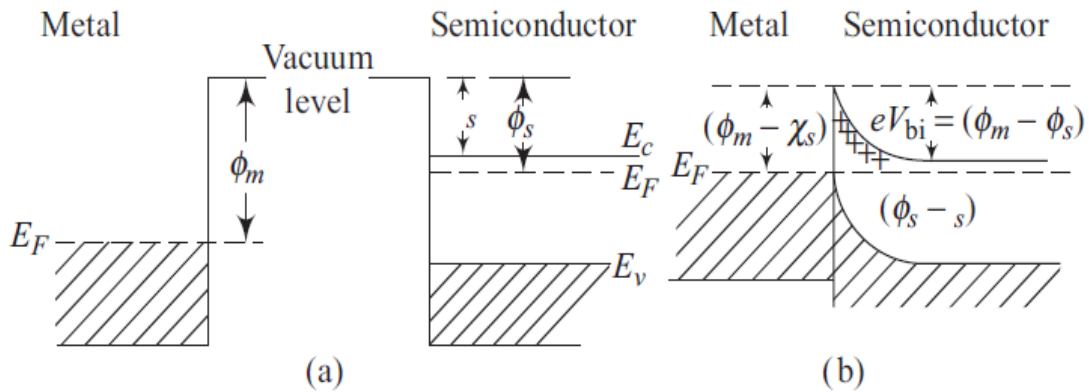


Figure 3. 1 Energy band diagram for metal and n-type semiconductor if $\phi_m > \phi_s$ (a) before contact, (b) after contact at thermal equilibrium and produce rectifier contact.

3.3.1. Rectifier contact

When the work function of metal is greater than work function of semiconductor, $\phi_m > \phi_s$, rectifier contact is formed for n-type semiconductors, in contrast, for p-type semiconductors just reverse above statement (Bhattacharya, 2013). Figure (3.1) a represents flat band diagram for both metal and n-type semiconductor before formation of contact. As shown in the figure, the Fermi energy level of semiconductor is at higher than that of metal. Thus, electrons in semiconductor easily diffuse to the metal side, because they have a higher energy. As electrons move to metal side, they left positive ions in semiconductor region. They generate negative ions in metal region, this process

will be continue up to both Fermi levels are aligned in such state. After that, the movement of electrons from semiconductor to metal does not take place, because the positive and negative ions create a barrier that blocks flow of electrons. Positive and negative ions produce an electric field, eventually this electric field prevents the diffusion of electrons from semiconductor into metal side. In order to overcome this barrier, a potential is required. The minimum voltage required to flow charge carriers is called built in voltage at thermal equilibrium state seen from Figure (3.1)b.

Built in voltage for n-type can be expressed as follow (Williams, 1983):

$$eV_{bi} = \phi_m - \phi_s \quad (3.1)$$

where e is electronic charge, V_{bi} is built in voltage, ϕ_m is metal work function and ϕ_s is semiconductor work function.

Also barrier height for n-type can be expressed as the difference between the work function of metal and the electron affinity of semiconductor as shown in below (Mönch, 1994):

$$e\phi_{Bn} = e(\phi_m - \chi_s) \quad (3.2)$$

And for p-type barrier height expressed as

$$e\phi_{Bp} = E_g - e(\phi_m - \chi_s) \quad (3.3)$$

where ϕ_{Bn} is barrier height for n-type semiconductor, χ_s is electron affinity of semiconductor and ϕ_{Bp} is barrier height for p-type semiconductor

If forward bias voltage is applied on the device, barrier is getting lower, then the electric field is reduced. Therefore, flowing of electrons starts again when the applied voltage equals to built in voltage. According to Fermi-Dirac distribution, there is only a fraction of charges has sufficient energy to cross barrier. Thus, as the applied voltage increases, the barrier height becomes lower.

The number of electrons that have ability to overcome the barrier exponentially increases. The resulted current is called thermionic emission current, and it is mathematically expressed as follows (Aslan et al., 2019):

$$I = AA^*T^2 \exp\left(-\frac{e\phi_B}{k_B T}\right) \exp\left[\left(\frac{e(V - IR_s)}{nk_B T}\right) - 1\right] \quad (3.4)$$

where, n is ideality factor, and I_0 is the saturation current, and I_0 is described as (Turut et al., 2015):

$$I_0 = AA^*T^2 \exp\left(-\frac{e\phi_B}{k_B T}\right) \quad (3.5)$$

where A is the effective contact area ($5.024 \times 10^{-3} \text{cm}^2$), A^* is the Richardson constant ($112 \text{Acm}^{-2} \text{K}^{-2}$) for n-Si.

3.4. Electrical Parameters of Metal-Semiconductor Contact

Here we will discuss some basic of electrical parameters of metal-semiconductor contact, such as ideality factor, series resistance and barrier height. Those parameters are brick for investigation of electrical properties of devices.

3.4.1. Ideality factor

Generally, ideality factor measures the quality and performance of diode. According to ideal diode equation, all charge carrier transitions take place from band to band or recombination occur via traps in bulk area of device, not in the junction interface. In practice, it is not possible in all times, because of may some recombination be take place in somewhere else except bands.

Typical value of ideality factor for diode is in the range between 1 to 2. However sometimes it exceed from this upper. There are many factors which cause diode to deviate from ideality and increases ideality factor such as interface states between semiconductor and metal, doping level in semiconductors, Schottky effect of barrier and generation & recombination process in space charge region (Ilke Tascioglu et al., 2014; Z. Çaldıran et al., 2013).

Ideality factor is important parameter because any change in ideality factor influence the performance of the diode (Einspruch and Cohen., 1988; Photodetectors n.d, 2015).

3.4.2. Series resistance

Series resistance in metal-semiconductor contacts provides all resistances at the interface layers equivalent to circuit. Generally, for obtain high performance in photo detector devices, it is needed low series resistance. As series resistance decreases the photocurrent and ideality factors are increase. Thus, the detectivity and photoresponsivity is increased with decreasing series resistance (Oksana Ostroverkhova, 2013).

3.4.3. Barrier height

Barrier height is defined as difference between edge of majority carriers and fermi level energy, Barrier height for n-type given in follows (Monch 1994) .

$$\phi_{Bn} = E_c - E_F \quad (3.8)$$

And Barrier height for p-type is given in follow:

$$\phi_{Bp} = E_F - E_v \quad (3.9)$$

It will be formed directly after metal and semiconductor make contact together. Barrier height is important parameter because it is responsible for charge conduction mechanism in contact and its capacitance manner . Barrier height is a function of interfacial layer, doping, type of metal and semiconductor.

Additionally, image force lowering leads to decrease barrier height. In the presence of interfacial layer, the barrier height will enhanced as shown in Fig.(3.3)

From Figure (3.3), The final expression of energy band diagram for metal and n-type semiconductor contact with an interfacial layer is written as below (Bhattacharya, 2013):

$$E_g - e\phi_o - e\phi_{Bn} = \frac{1}{eD_s} \sqrt{2e\epsilon_s N_d (\phi_{Bn} - \phi_n)} - \frac{\epsilon_i}{eD_s \delta} [\phi_m - (\chi_s + \phi_{Bn})] \quad (3.10)$$

where ϕ_o is barrier height at zero potential, D_s is density of states per cm^2 per eV, ϵ_s is dielectric constant of semiconductors, ϵ_i is dielectric constant of interfacial layer, N_d is donor concentrations and δ is interfacial layer thickness.

By applying two assumptions

First, there are a continues and large number of density of states across bands, so it can be assume $D_s \rightarrow \infty$, then Equation (3.10) becomes

$$\phi_{Bn} = \frac{1}{e}(E_g - e\phi_o) \quad (3.11)$$

The equation (3.11) yields that barrier height is not dependent on some material parameters like work functions and electron affinity likewise barrier height is a function of energy band gap and surface energy.

Second, interfacial layer is very thin, when multiply by density of states, can be neglected, let assume $D_s \delta \rightarrow 0$

Equation (3.10) become

$$\phi_{Bn} = (\phi_m - \chi_s) \quad (3.12)$$

Notice that equation (3.12) exact the same of the equation (3.2)

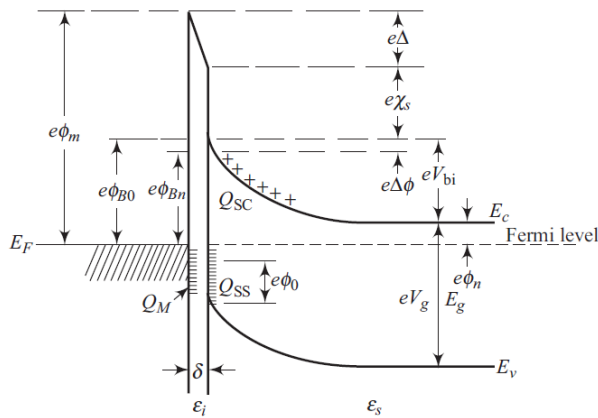


Figure 3. 2 Energy band diagram for metal–(n-type) semiconductor junction with interfacial layer.

3.5. Photo-Sensing Parameters of Photodetector

Photodetectors are devices which transform light energy to electrical energy. When electron in the valence band absorbs light energy and is transferred to conduction band, it leaves valence band. Therefore, free electron-hole pairs will be generated which both of them contribute in current conduction mechanism. There are many types of photosensing devices such as photodetectors, photovoltaics, photodiodes and phototransistors.

In this section, a brief explanation and description are given, for some important photosensing parameters of photodiode such as responsivity, detectivity and linear dynamic range (LDR).

3.5.1. Responsivity

Responsivity defines the ratio of photocurrent produced per optical incident illumination power of light, and it is measured in unit A/W and expressed as follows (Hammond, 2013):

$$R = \frac{I_{ph}}{PA} \quad (3.13)$$

where R is responsivity, I_{ph} is photocurrent, P is illuminated power and A is illuminated area. Responsivity also varies with biasing voltage, temperature, power of incident light, and illumination area, energy gap of semiconductor and barrier height of Schottky contact.

In metal-semiconductor contact, photocurrent can be produced by two ways:

- (i) absorption of energy of incident light if $h\nu > E_g$ satisfies
- (ii) the generation of hot carriers in metal by internal photoemission process.

3.5.2. Detectivity

The detectivity represents the ability of photodiode for observing small light signals. In SI system, it measures in unit (Jones). Mathematically expressed as below (Tang, 1986):

$$D^* = \frac{R}{\sqrt{2eJ_{dark}}} \quad (3.14)$$

where D^* is specific detectivity.

For obtain high detectivity it is necessary high responsivity and low noise current, a fraction of noise current comes from dark current so as the dark current decrease the detectivity increase.

3.5.3. Linear dynamic range

Linear dynamic range in photodiode is measure the linearity produced photocurrent per incident illumination power (i.e measure the photosensing linearity of photodiode). To study of variation linear dynamic range as a function of reverse voltage under various illumination intensities, the below equation can be used:

$$LDR = 20 \log\left(\frac{J_{ph}}{J_{dark}}\right) \quad (3.15)$$

where LDR is linear dynamic range, J_{ph} is photocurrent density and J_{dark} current density at dark.



4. EXPERIMENTAL PROCEDURE

In this section, the fabrication of the diode will be described in detail. The first step in the device fabrication was cleaning the silicon wafer via RCA method. After that the ohmic contact prepared on silicon wafer using thermal evaporation technique. In the third step the deposition of organic layer is done via spin coater machine. Finally, the front contact is formed using thermal evaporation technique. C-V and I-V measurements were taken for the sample with and without organic layer in dark and under solar simulator with power between 30-100 mW/Cm².

4.1. Silicon Wafer Cleaning

The device performance and reliability strongly depend on the ratio of the chemical and special impurities on the substrate. The main purpose of the cleaning wafer. It is to remove all chemical contaminants and impurities, which effect on devices performance, There are many methods to clean sample such as dry-physical, wet-chemical and vapor phase. First step is clean silicon wafer, (100) orientation and 1-10 Ωm resistivity, with Radio Corporation of America technique (RCA). RCA technique is developed by W. Kern. It is useful for cleaning substrate from organic and ionic contaminations as well as removing oxide layer if it is needed. RCA cleaning totally consists of four steps two of them are basics and others are optional steps. In this study all steps are performed and between each two steps silicon substrate was washed and rinsed in deionized water using ultrasonic device. The whole steps are given in the Table (4.1). RCA cleaning is necessary to be done before high temperature processing.

4.2. Formation of Ohmic Ontact

After cleaning n-Si substrate and Au metal by alcohol and deionized water, silicon substrate put into thermal evaporation machine then Au metal evaporated to unpolished side of silicon substrate under pressure 10⁻⁶ Torr as given in fig. (4.1), and

after that to get high quality ohmic contact thermal annealing was done for 3 min at 570 C° in nitrogen atmosphere the annealing furnace used for this purpose shown in Figure(4.2).

Table 4. 1 RCA cleaning steps

	process	ratio	temperature	period	Repetition
1.	Rinsing in deionized water			5 Minutes	2 times
2.	Trichlorethylene wash			5 Minutes	
3.	Tinsing in deionized water			5 Minutes	2 times
4.	Acetone wash			5 Minutes	
5.	Rinsing in deionized water			5 Minutes	2 times
6.	Methanol wash			5 Minutes	
7.	Rinsing in deionized water			5 Minutes	2 times
8.	Isopropyl wash			5 Minutes	
9.	Rinsing in deionized water			5 Minutes	2 times
10.	NH₄OH₄:H₂O₂:H₂O	(1:1:5)- (1:1:50)	40°C-75°C	3-10 Minute	
11.	Rinsing in deionized water			5 Minute	2 times
12.	HF:H₂O	(1:10)- (1:25)	25°C	0.5- 1 Minute	
13.	Rinsing in deionized water			5 Minute	2 times
14.	HCl:H₂O₂:H₂O	(1:1:6)- (1:1:50)	40°C-75°C	3-10 Minute	
15.	Rinsing in deionized water			5 Minute	2 times
16.	HF:H₂O	(1:10)- (1:25)	25°C	0.5- 1 Minute	
17.	Rinsing in deionized water			5 Minute	4 times
19.	Drying in (N ₂) Nitrogen gas			Enough time	



Figure 4. 1 Thermal evaporation machine used to evaporate metal.



Figure 4. 2 Furnace used for thermal annealing.

4.3. Deposition of Organic Layer Thin Film

The Brilliant blue ($C_{45}H_{44}N_3O_7S_2Na$) was bought from Sigma-Aldrich company, was used as an organic layer, First of all, Brilliant blue dissolved in methyl alcohol with

molarity of $1 \times 10^{-2} \text{ Mol.L}^{-1}$. Using the spin coating technique, Brilliant blue is coated on the front side of the silicon using precursor solution dropped onto the silicon side and silicon substrate rotate at 2000 rpm for 1 min inside the spin coater. Spin coating apparatus is shown in figure (4.3).



Figure 4. 3 Spin coater used to deposit organic thin film layer.

4.4. Formation of Rectifier Contact

Final step of fabrication process is forming rectify contact, In this part, Cu metal was evaporated onto the deposited organic film on the silicon substrate by helping circular shapes of shadow mask with radius of 0.4 cm. Fabricated device was depicted in figure (4.4).

4.5. Analyzing Method

To investigate electrical behavior of Cu/n-Si/Au and Cu/BB/n-Si/Au diodes (I-V) and (C-V) measurements were performed in dark and at room temperature.

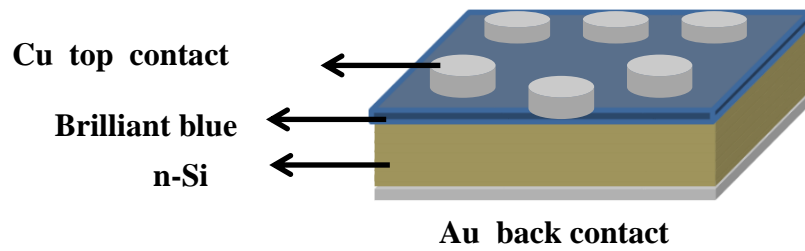


Figure 4. 4 Schematic diagram of Cu/BB/n-Si/Au.

Keithley 2400 source meter and HP agilent 4294A impedance analyzer are shown in figure (4.5) and figure (4.6), respectively.



Figure 4. 5 Keithley 2400 source meter.

Furthermore (C-V) measurement was carried out for different frequencies to know the quality performance of device.

In additional, for studying photo sensing properties, (I-V) measurements were taken under solar simulator with intensity power range between 30-100mW/cm² using of solar simulator.



Figure 4. 6 HP agilent 4294A impedance analyzer.

5. RESULTS AND DISCUSSION

In this section, Cu/n-Si/Au diode was prepared via thermal evaporation and spin coating methods with and without Brilliant blue as an organic interlayer. Then current-voltage and capacitance-voltage measurements were performed in dark and under solar simulator with intensity range 30-100 mW/cm² to investigate electrical and photoelectrical parameters of the organic based hybrid structure diode to compare with conventional diode.

In this chapter, all results related to the experimental data of prepared samples are given and discussed in detail.

5.1 Current-Voltage Measurement For Diodes Under Dark

Current-voltage measurements are one of the commonly used and effective method to study and analyze the electrical property of diode. Figure (5.1) shows semi-logarithmic current-voltage scale for Cu/n-Si/Au and Cu/BB/n-Si/Au devices in dark. It can be realized from Figure 5.1 that both diodes have rectification property, however, organic dye based one has higher rectification ratio than the other device. In other word, organic interfacial layer enhances the rectification property of the diode. As indicated in Figure (5.1), at low positive voltages, which is approximately less than 0.3 V, current is directly proportional to the forward biasing voltage. As applied voltage becomes higher, current exponentially varies with the voltage. Eventually, the graph curvature is downward (i.e saturated) due to the presence of series resistance in forward biasing while it is revealed a small saturation current and low dependency on voltage in reverse bias.

Semi-logarithmic current-voltage of Figure 5.1 obeys thermionic emission equation with presence of series resistance which is given below (Ebisawa et al.,1983):

$$I = AA^*T^2 \exp\left(-\frac{e\phi_b}{k_B T}\right) \exp\left[\left(\frac{e(V - IR_s)}{nk_B T}\right) - 1\right] \quad (5.1)$$

where, I_0 is the saturation current, and expressed as (Liu et al., 2018):

$$I_0 = AA^*T^2 \exp\left(-\frac{e\phi_b}{k_B T}\right) \quad (5.2)$$

It is clear that ideality factor can be defined from the thermionic emission the Eq. (5.1) and barrier height is calculated using the saturation reverse current Eq. (5.2).

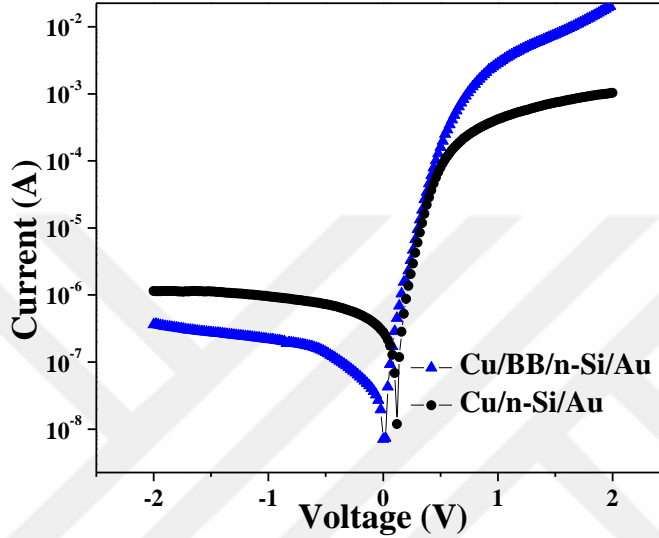


Figure 5. 1 Semi-logarithmic I-V plots for Cu/BB/n-Si/Au and Cu/n-Si/Au diodes in dark.

$$n = \frac{e}{k_B T} \frac{dV}{d \ln(I)} \quad (5.3)$$

And

$$\phi_b = \frac{k_B T}{e} \ln\left(\frac{AA^*T^2}{I_0}\right) \quad (5.4)$$

With the help of Eq. (5.3), ideality factors are determined for prepared samples, which are presented in Table 5.1. The values are 1.5 and 1.3 for Cu/n-Si/Au and Cu/BB/n-Si/Au diodes, respectively. Ideality factor is unity for ideal diode. This increasing may be due to inhomogeneity of interface states and presence of series resistance (Ghahramani et al., 2012). The ideality factor value of the organic-based diode has smaller than that of device without BB layer. So, organic based one represents better performance.

Also using Eq. (5.4) at zero bias-voltage, The barrier height were measured and tabulated in Table 5.1 Their values are 0.75 and 0.82 eV for Cu/n-Si/Au and Cu/BB/n-Si/Au junctions, respectively. As seen, the barrier height becomes higher as the organic interfacial layer added to metal semiconductor interface. Also, this feature can be recognized from plots. Diode with higher barrier height (i.e organic based dye diode) exhibits better rectification property. This can be evaluated as a result of discourage of silicon bonds after inserting organic layer because charge transportation in organic semiconductors can be localized, or organic interlayer can form dipole between semiconductor metal surfaces leading to change in permittivity. Also, image force lowering effect on barrier height.

It is well known fact that series resistance is important parameter in electrical devices. Series resistance directly effects on quality, reliability and stability of devices. It is possible to obtain more about series resistance by applying Cheung functions as given in below (Bera et al., 2008):

$$\frac{dV}{d \ln I} = \frac{nk_B T}{e} + IR_s \quad (5.5)$$

And

$$H(I) = IR_s + n\Phi_B \quad (5.6)$$

H(I) given as follows:

$$H(I) = V - \frac{nk_B T}{e} \ln\left(\frac{I}{AA * T^2}\right) \quad (5.7)$$

By applying Eq. 5.5 gives out a line as shown in Fig. 5.2. For both diodes from this line, the R_s is directly obtained the slope. The ideality factor is also can be determined from y-intersection of this line by applying Eq. 5.5.

The values obtained from Eq. 5.5 are inserted in Table 5.1. The values for ideality factors are 1.52 and 1.03, and values for series resistances are 1166.7 and 405 Ω for Cu/n-Si/Au and Cu/BB/n-Si/Au heterojunctions, respectively.

Also, by using Eq.5.6, H(I) versus I shows linear behavior as shown in Figure 5.3 for both diodes. The slope of the line is equivalent to R_s , and y-intersection of the line gives the barrier height. The values are tabulated in Table 5.1. The calculated barrier heights are 0.77 and 0.84 eV, and series resistances are 1320 and 437 Ω for Cu/n-Si/Au and Cu/BB/n-Si/Au diodes respectively.

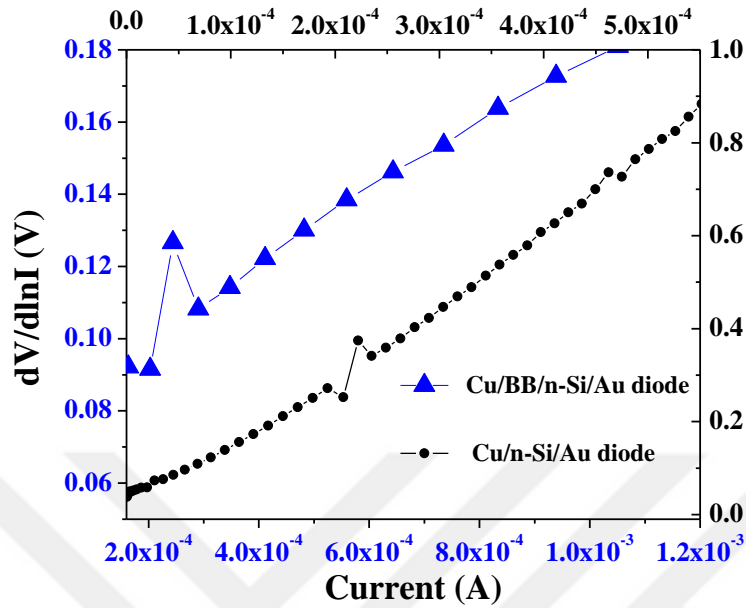


Figure 5. 2 $dV/d\ln I$ versus I for Cu/n-Si/Au and Cu/BB/n-Si/Au diodes.

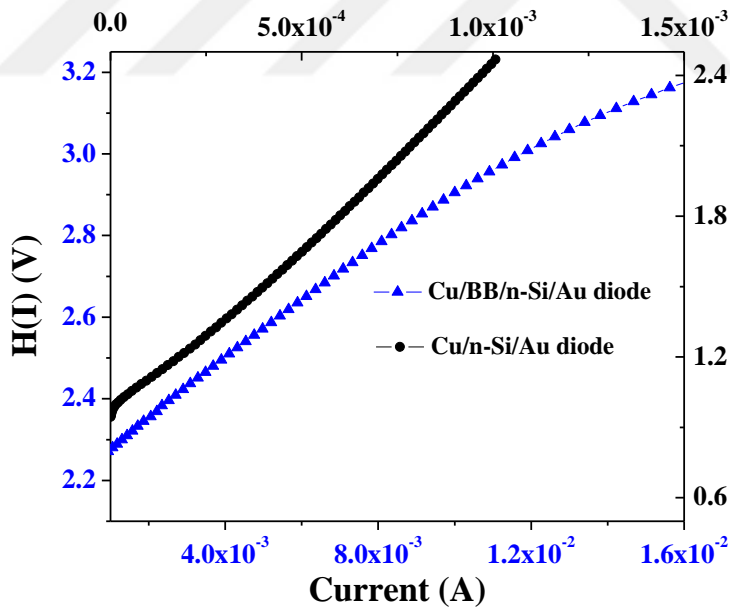


Figure 5. 3 $H(I)$ versus I plots for Cu/n-Si/Au and Cu/BB/n-Si/Au diodes.

There is a good agreement between measured and calculated current-voltage measurement plot and Cheung function plots, Although, a little difference can be noticed, and this little difference is acceptable. In fact, series resistance is a current

limiting factor, lower series resistance allows more current to pass through metal-semiconductor junction. When the current is rising (i.e. lower series resistance), it leads to higher rectification ratio in devices. This description exact coincident, with our results. In this study, the diode without organic layer has higher series resistance and lower rectification property than diode with organic interfacial layer.

Furthermore, modified Norde's function was used to study more about series resistance and barrier height as shown in Figure (5.4). The modify Norde's function can be expressed as below (Demirezen et al., 2012):

$$F(V) = \frac{V}{\gamma} - \frac{k_B T}{e} \ln\left(\frac{I(V)}{AA^* T^2}\right) \quad (5.8)$$

where γ is a first integer greater than ideality factor of diode

And electrical parameters, extracted with helping of two equations:

$$\phi_b = F(V_{\min}) + \frac{V_{\min}}{\gamma} - \frac{k_B T}{e} \quad (5.9)$$

$$R_s = \frac{k_B T(\gamma - n)}{e I_{\min}} \quad (5.10)$$

where $F(V_{\min})$ is the minimum value of $F(V)$, V_{\min} is the corresponding voltage value for $F(V_{\min})$. I_{\min} is the current corresponding to the voltage (V_{\min}) in I-V characteristics data.

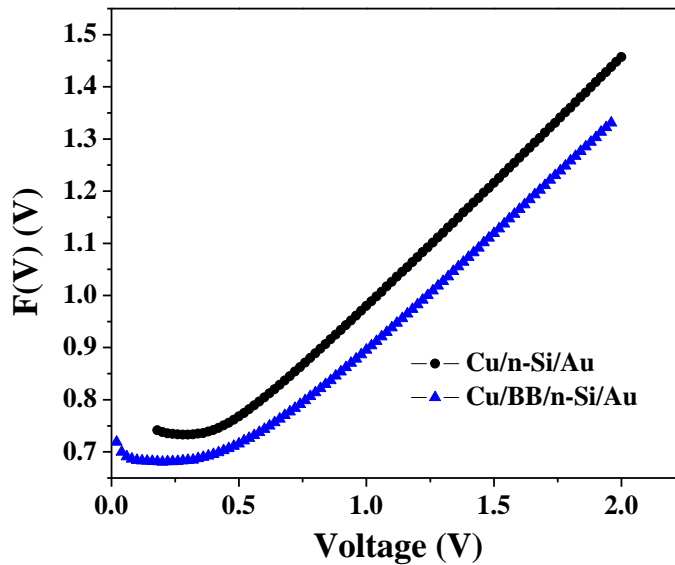


Figure 5. 4 Norde's function plots for Cu/n-Si/Au and Cu/BB/n-Si/Au diodes.

Using Eq.5.9, barrier height values were determined as 0.7 and 0.75 eV for Cu/n-Si/Au and Cu/BB/n-Si/Au diodes, respectively. series resistance values were yielded from Eq. 5.10 as 5116 and 2095 Ω for Cu/n-Si/Au and Cu/BB/n-Si/Au diodes respectively. The values are tabulated in Table 5.1.

From the Table 5.1, the values of R_s obtained from Norde's function is greater than that of Cheung functions. This may be related to different nature of each methods. From Cheung functions and Norde function, the series resistance of the sample without organic layer is greater than in organic based diode. This may be due to existence of thin oxide layer on silicon in MS interface. After removing contaminants, the oxide layer may be produced, because oxygen is very active to interact with silicon (Kilicoglu et al., 2014; Sekhar Reddy et al., 2016).

Table 5. 1 Electrical parameters for Cu/n-Si/Au and Cu/BB/n-Si/Au diodes determined from I-V measurements

Sample	$\ln I-V$		$dV/d\ln I-V$		$H(I)-V$		$F(V)-V$	
	n	Φ_b (eV)	n	R_s (Ω)	Φ_b (eV)	R_s (Ω)	Φ_b (eV)	R_s (Ω)
Cu/n-Si	1.50	0.74	1.52	1166	0.77	1320	0.70	5116
Cu/BB/n-Si	1.36	0.83	1.03	405	0.84	436	0.75	2095

5.2 Capacitance – Voltage Measurement

To study and investigate the effect of the interface state density of Cu/n-Si/Au and Cu/BB/n-Si/Au diodes on their electrical behaviors, capacitance-voltage measurements were carried out in the frequency range between 250 kHz to 1500 kHz at room temperature for both diodes. Capacitance-voltage characteristics are presented in Figure (5.5) and Figure (5.6) for both Cu/n-Si/Au and Cu/BB/n-Si/Au diodes. As shown from the figures, almost reference diode exhibits little lower capacitance than dye diode. means that inserting organic layer, capacitance property of the metal - semiconductor diode is enhanced. Moreover capacitance is decreased with increasing of the frequency for both diodes. This may be explained as the result of sufficiently high frequency signal interface states block A.C signals, but low A.C signals can migrate through the interface of states easily (Baraz , 2017; Hüseyin and Yildiz, 2019).

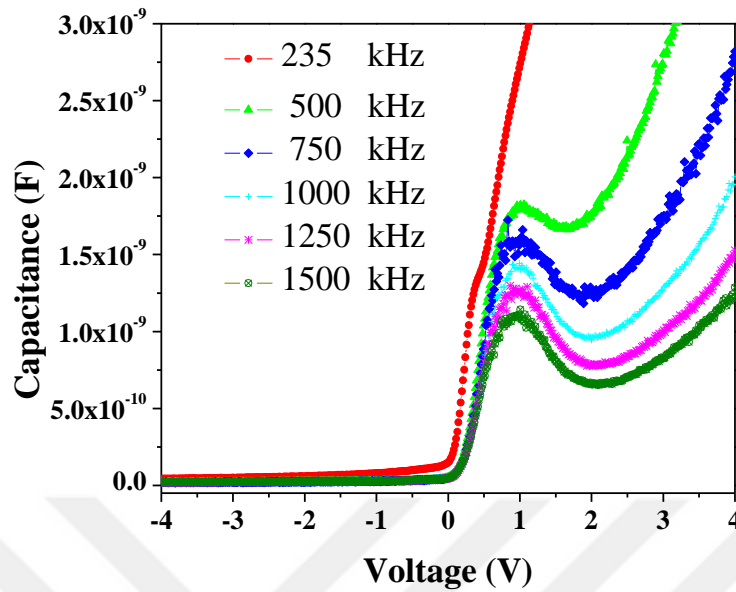


Figure 5. 5 Capacitance - voltage measurement for Cu/n-Si/Au diode at various frequencies.

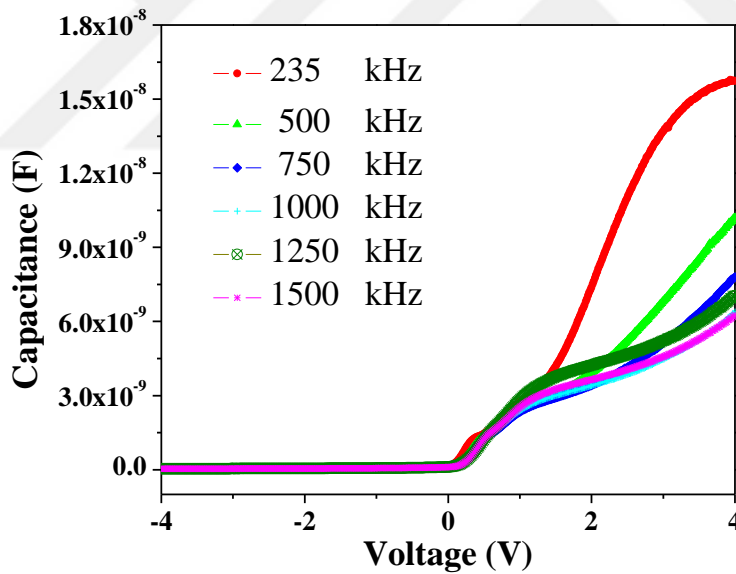


Figure 5. 6 Capacitance - voltage measurements for Cu/BB/n-Si/Au diode at various frequencies.

It can be noticed three different regions from Figure (5.5) from right to left and at various frequencies. The capacitive behavior is similar to MIS or MOS structure. There are three regions; first one is inversion region in which the capacitance is either almost constant or decreases slowly with voltage. Second one is the depletion region in

which capacitance started to decrease suddenly with voltage. The last one is accumulation region with a constant part of the plot. The presence of interface layer can be caused deviate from common case as shown in Figure (5.6). The three different regions cannot be distinguishable from each other very well for organic based devices.

$C^{-2} - V$ plot is one of the useful method to determine some electrical parameters, plot is linear at low reverse voltages approximately up to -1 volt as shown in Figure(5.7) and figure (5.8) for Cu/n-Si/Au and Cu/BB/n-Si/Au structures respectively. and the calculated values are presented in Table 5.2. In this reverse depletion region capacitance can be expressed as follows (Arife Gencer Imer, 2016):

$$C^{-2} = \frac{2(V_{bi} + V)}{e\epsilon_s\epsilon_o A^2 N_d} \quad (5.11)$$

Table 5. 2 Electrical parameters for Cu/n-Si/Au and Cu/BB/n-Si/Au diodes determined from C-V measurements

Sample	Φ_b (eV)	V_{bi} (V)	E_F (eV)	$N_d \times 10^{14}(\text{cm}^{-3})$
Cu/n-Si	0.78	0.51	0.28	4.9
Cu/BB/n-Si	0.82	0.60	0.23	37.7

By applying Eq. (5.11) on the Figure (5.6) built in voltage and donor concentration calculated from the slope and intersection. The obtained values for built in voltage are 0.52 and 0.60 V for reference and dye diodes, respectively.

Fermi level can be determined by using the relation below (Fetouhi et al., 2014):

$$E_F = \frac{K_B T}{e} \ln\left(\frac{N_v}{N_a}\right) \quad (5.12)$$

It is possible to determine the value of barrier height using the equation below (H. Kim,. 2017):

$$\phi_{B(C-V)} = V_{bi} + E_F \quad (5.13)$$

Calculated values for barrier heights are 0.77 and 0.82 V for Cu/n-Si/Au and Cu/BB/n-Si/Au diodes, respectively. This confirms the results obtained from I-V measurements and stated that inserting organic layer, the barrier height is increased. Although the values determined from Capacitance-voltage measurements are higher than the values determined from Current-Voltage measurements. This may be as a result

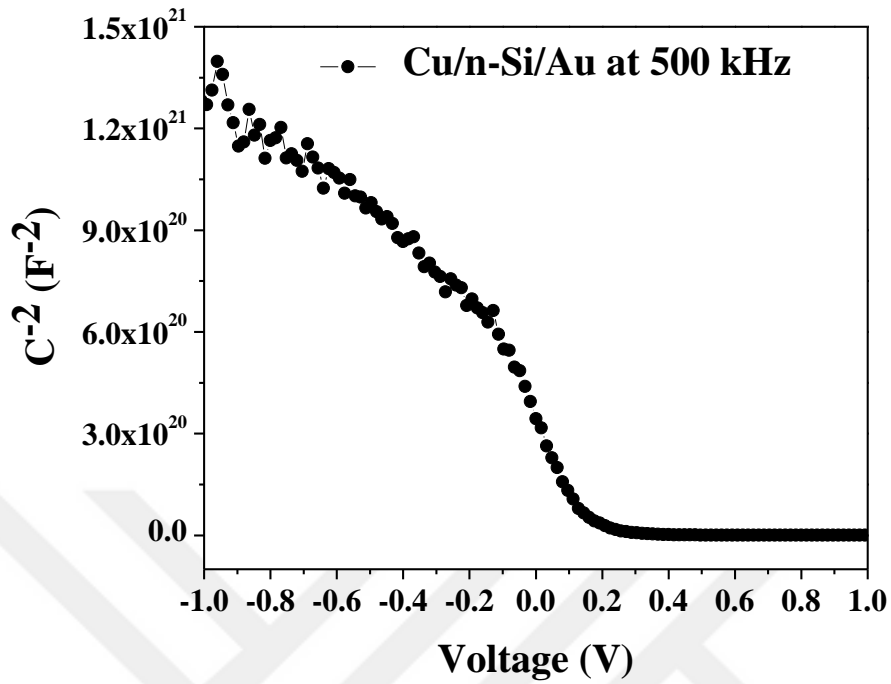


Figure 5. 7 Reverse C^{-2} -V characteristic for Cu/n-Si/Au diode in room temperature and at 500 kHz.

of presence organic and oxide layer at the interface, inhomogeneities in interface states as well as effect of image force barrier lowering (Shtrikman, 2009).

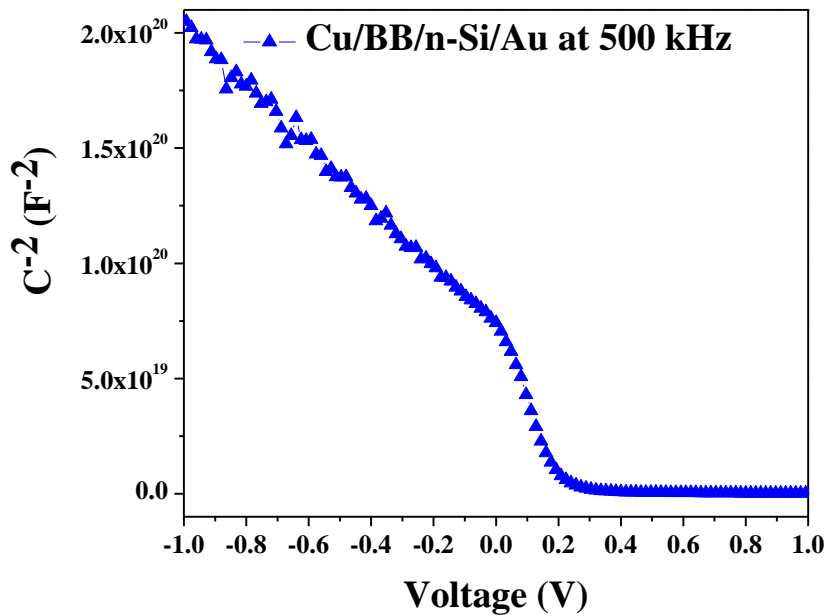


Figure 5. 8 The C^{-2} -V characteristic for Cu/BB/n-Si/Au diode in room temperature and at 500 kHz.

5.3 Photoelectrical Properties of Cu/BB/N-Si/Au Photodiode

Figure (5.9) shows forward and reverse bias semilogarithmic current-voltage plots of Cu/BB/n-Si/Au structure in dark and under different light illuminations produced by a solar simulator at room temperature. The diode presents a good rectifier behavior in dark and under illuminations with rectification ratios 19.43 and 24.74 in dark and under illumination respectively at $\pm 2 V$. Current in forward bias independent of light intensity, but exponentially a function of applied voltage, while in reverse bias current rapidly increase as the light intensity increase. This phenomena is due to the fact that in the reverse bias depletion region is extended as light exposed to the junction and generate electron-hole pairs are created by absorption of photon, Then revers bias voltage provides sufficient energy to accelerate of electron-hole pairs towards positive and negative electrodes thus generated electron-hole pairs contribute conduction mechanism, and cause to increase reverse current. In addition, the photodiode exhibit photo response properties.

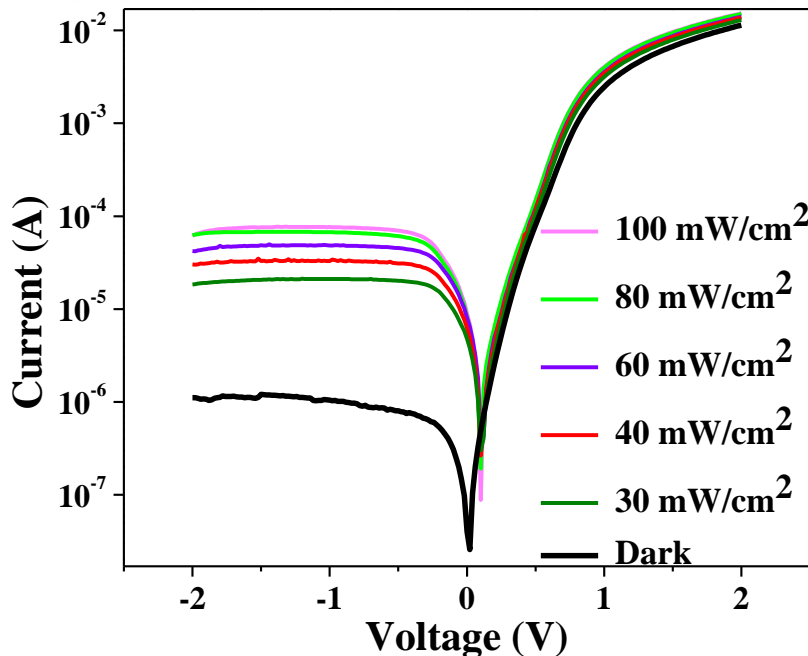


Figure 5. 9 Reverse and forward bias lnI-V plots of Cu/BB/n-Si/Au photodiode in dark and under various illuminations at room temperature.

To understanding more about the photocurrent dependency on illumination power of prepared structure and analyzing of its photo sensing property the below relation can be used (Ocaya et al., 2016):

$$I_{ph} = \alpha P^\gamma \quad (5.14)$$

It is given in Figure (5.10) , the value of the exponent γ can be determined from the slope of double logarithmic I-P plots for each voltage. The γ values were found to be as 1.13, 1.50, 1.40, 1.60 and 1.75 for -0.1,-0.5,-1,-1.5 and -2 biasing voltages respectively. The results indicate that the variation of photocurrent with incident illumination power is almost linear. So, it is evidence for continues arrangement of existing localized states.

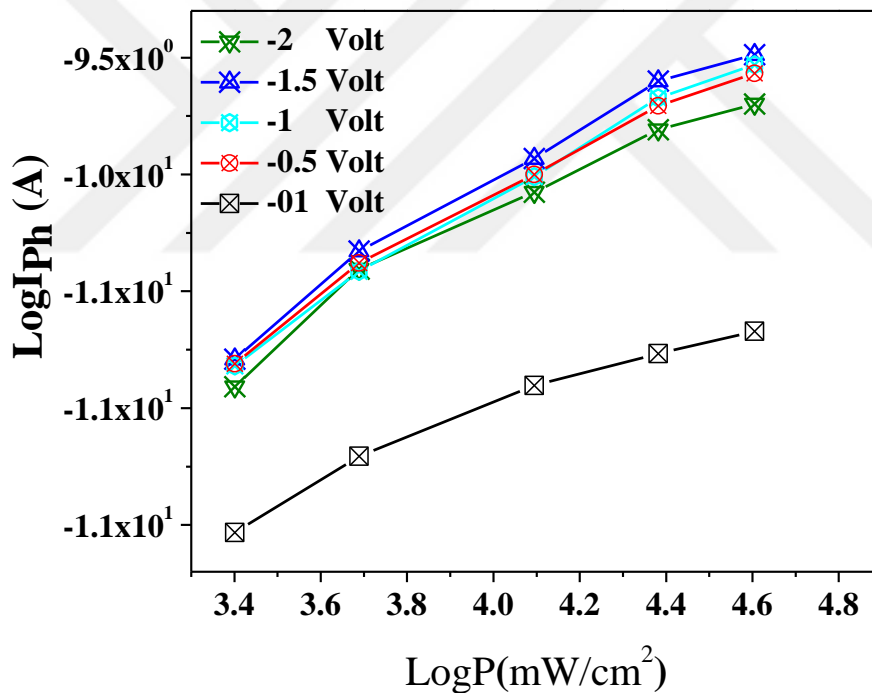


Figure 5. 10 The relation between LogIph versus LogP at various reverse biasing voltages for Cu/BB/n-Si/Au photodiode.

The linear variation of photocurrent versus illumination power is shown in figure(5.11). This is the evident for the relation between incident power and produced photocurrent, that is almost linear with illumination power ($P < 80 \text{ mW/cm}^2$), But when incident power intensity exceeds 80 mW/cm^2 , non-linear region begins and

photocurrent is saturated for intensities greater than 80 mW/cm^2 . This may be due to the presence of a great number of electron-hole pairs at the junction. Thus, no more photons will be capable of being absorbed in the junction, this behavior makes prepared photodiode suitable to use as a photosensor in small biasing voltages to detect low amount of intensity signals.

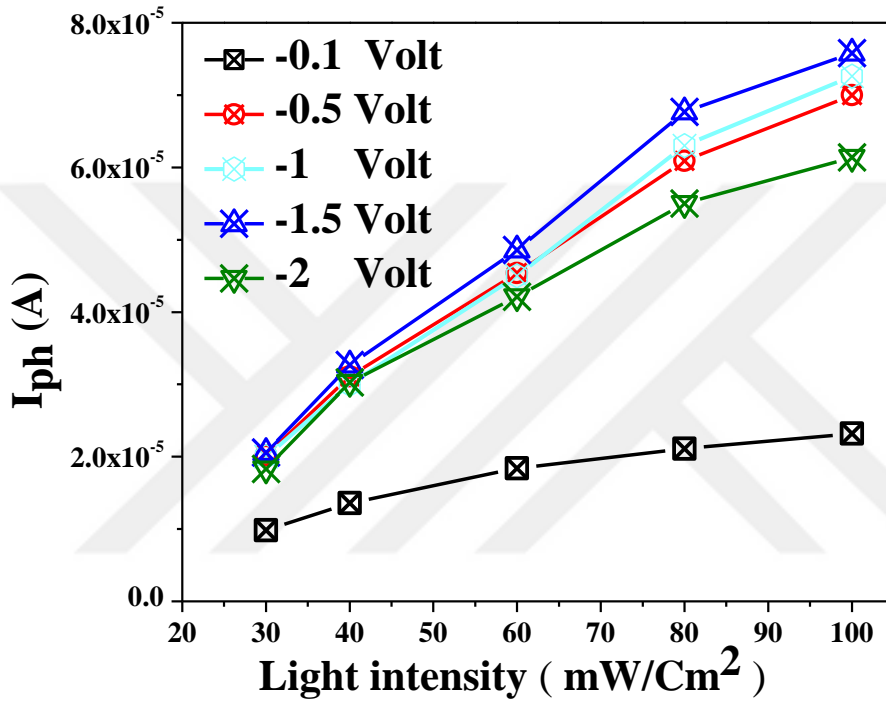


Figure 5. 11 The relation between photocurrent and incident power at various reverse biasing voltages for Cu/BB/n-Si/Au photodiode.

Responsivity is a measure of photodiode effectiveness for incident light, expressed by the following relation:

$$R = \frac{J_{ph}}{P} \quad (5.15)$$

Figure (5.12) represents photoresponsivity as a function of reverse biasing voltages under different illuminations for Cu/BB/n-Si/Au photodiode. It is clear from figure (5.12) that photoresponsivity depends on reverse voltage biasing: As reverse voltage bias increases, the photoresponsivity increases rapidly.

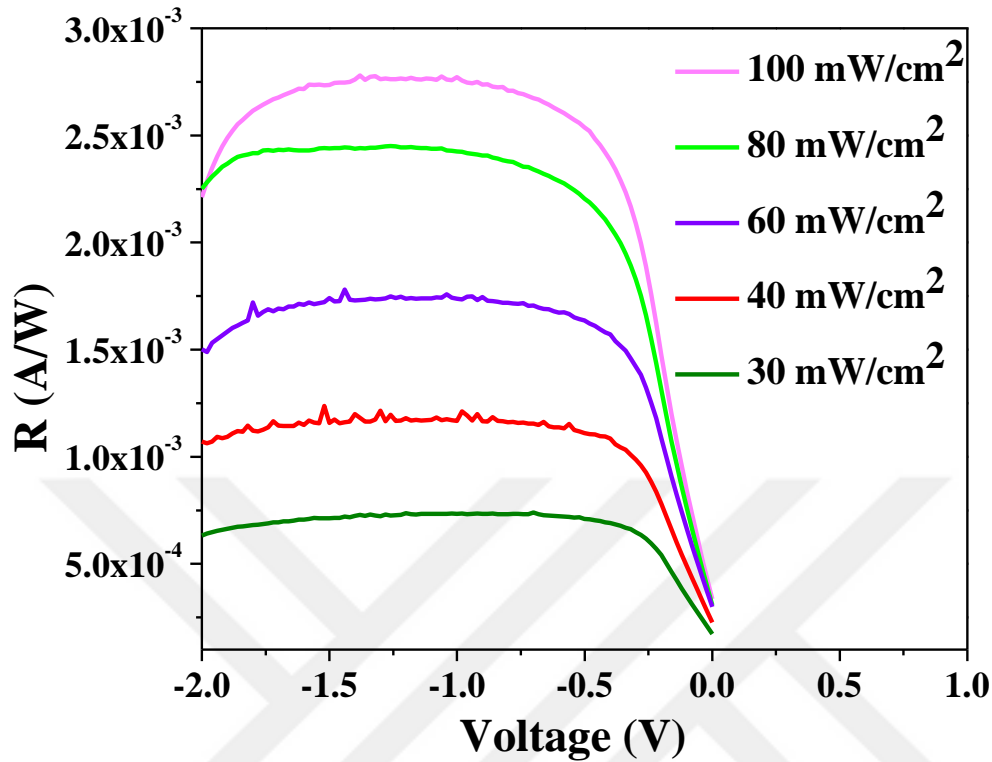


Figure 5. 12 Photoresponsivity as a function of reverse biasing voltages under different illuminations for Cu/BB/n-Si/Au photodiode.

In addition, it is revealed that the different light intensities can be distinguishable for all reverse biasing voltages range approximately $V_R > 0.3$ V. Thus, This is good characteristic of new generated photodiode, that have to use in optoelectronic applications.

Additionally, it is obvious that the responsivity of fabricated photodiode is almost at high enough reverse bias voltage region.

To measure the capacity of a prepared photodiode to identify wavelengths of incident, light the detectivity is calculated by applying the following formula:

$$D = \frac{R}{\sqrt{2eJ_{dark}}} \quad (5.16)$$

It is measured unit in $(cm \cdot Hz^{\frac{1}{2}}/w)$, and expressed by Jones.

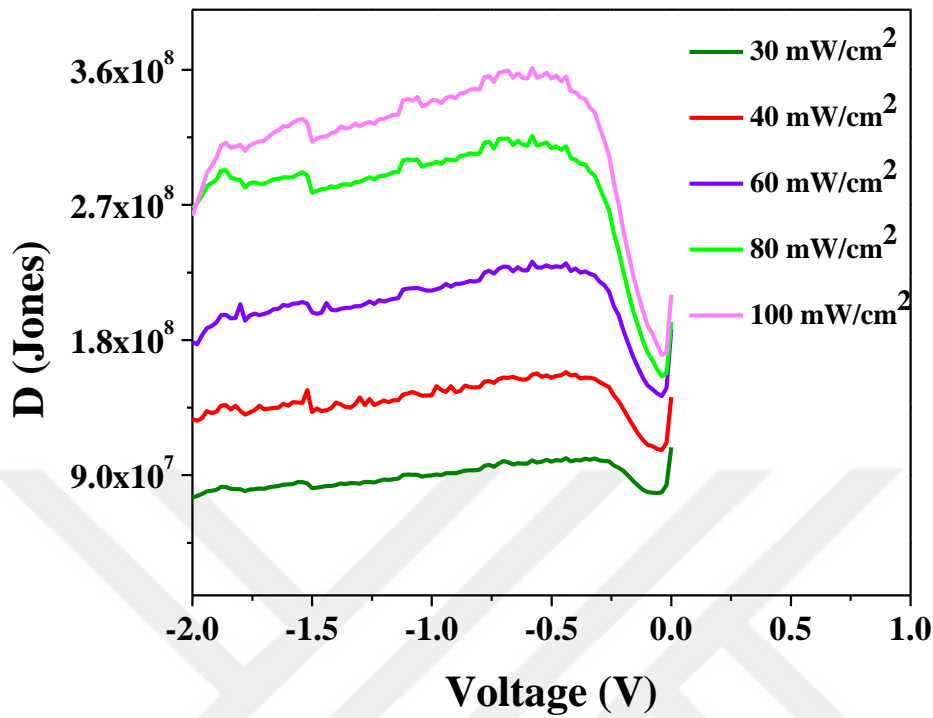


Figure 5. 13 The variations detectivity with respect reverse bias voltage for Cu/BB/n-Si/Au photodiode under various light intensities.

Figure (5.13) represents the variation of detectivity with respect to reverse bias voltage for Cu/BB/n-Si/Au photodiode under various light intensities. It is clear that the detectivity increases for small voltage values up to 0.3 Volt. beyond 0.3V, remains stable for all illumination intensities. In addition, it is clear that the prepared photodiode can detects small signals of incident light.

To study of variation linear dynamic range as a function of reverse voltage under various illumination intensities, the below formula was used:

$$LDR = 20 \log \left(\frac{J_{ph}}{J_{dark}} \right) \quad (5.17)$$

The variation linear of dynamic range with respect to reverse bias voltage is shown in Figure (5.14). It is clear that linear dynamic range rapidly increase with increasing reverse voltage After 0.3 V, it lineary enhances with the reverse voltage.

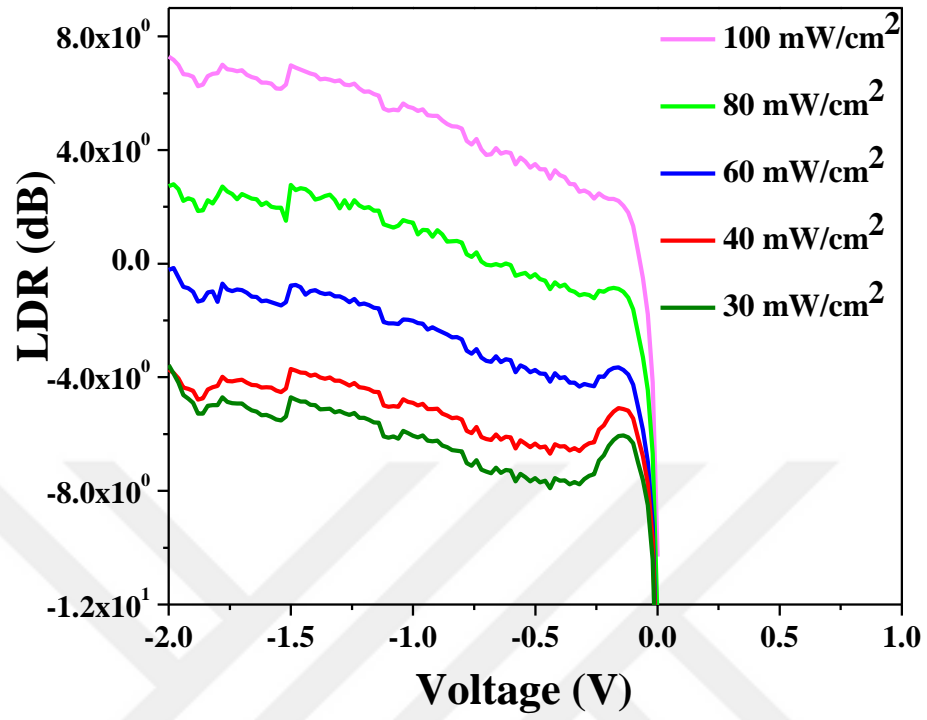


Figure 5. 14 The variations of linear dynamic range with respect of reverse bias voltage.



6. CONCLUSION

In this study, metal-semiconductor contact with and without organic interlayer were fabricated. The Au metal was evaporated on n-Si substrate using thermal evaporation technique, then thermal annealing treatment was performed to obtain ohmic contact. After dissolving organic material in alcohol, it was deposited on n-Si wafer via spin coating method. For formation of rectifier contact, Cu metal was evaporated to the film.

The current-voltage measurements were used to extract the electrical parameters of Cu/n-Si/Au and Cu/BB/n-Si/Au devices such as ideality factor, barrier height and series resistance using different methods like thermionic emission theory, Cheung functions and modified Norde method. The obtained values are presented in Table 5.1. According to obtained results, the electrical parameters of device were improved by inserting organic interlayer, and show better rectification behavior with higher barrier height. Additionally, frequency dependent capacitance-voltage measurements were done at room temperature and frequency range from 235 kHz to 1500 kHz. The results show that at sufficient high frequencies, the interface cannot flow A.C signals. Furthermore, some electrical parameters like barrier height, built in voltage, Fermi energy level and donor concentration were calculated from C^{-2} -V plot at 500 kHz for both Cu/n-Si/Au and Cu/BB/n-Si/Au devices.

Current-voltage measurements under different illuminations range from 30 to 100 mW/cm² were taken. The determined results indicate that the fabricated photodiode has a good photocurrent response to incident light intensity with respect to reverse biasing voltage. Also, the fabricated photodiode has high photo responsivity for incident power of illumination, and it has ability to detect small signals of incident light at low reverse voltages.

As a result, the fabricated device is good candidate to be used in electrical and optoelectrical applications such as photodiode.



REFERENCES

- Abdelhalim, Z., 1996. *Electronic Devices*. Dar El hakeem press,Caro.
- Abdel-Khalek, H., Shalaan, E., Mohamed, A. S., Ahmed, M. E., 2018. Effect of illumination intensity on the characteristics of Cu(Acac)₂/n-Si photodiode. *Synthetic Metals*, **245**: 223-236.
- Ali, U., Imer, A. G., Ocak, Y. S., 2015. Electrical and photoelectrical characterization of an organic-inorganic heterojunction based on quinoline yellow dye. *Materials Science in Semiconductor Processing* **39**: 569-574.
- Altuntaş, H., Altındal, Ş., Özçelik, S., and Shtrikman, H., 2009. Electrical characteristics of Au / n -GaAs schottky barrier diodes with and without SiO₂ insulator layer at room temperature. *Vacuum*, **83**: 1060-1065.
- Arca, F., 2013. *Organic Photodiodes For Industrial Sensing and Medical Imaging*. Technische universität münchen.
- Aslan, F., Hikmet, E., Fahrettin, Y., 2019. Electrical and fotoconducting characterization of al/coumarin:zno/al novel organic-inorganic hybrid photodiodes. *Journal of Alloys and Compounds*, **789**: 595-606.
- Baraz, N., Yücedağ, İ., Azizian-Kalandaragh, Y., 2017. Electric and dielectric properties of Au / ZnS-PVA / n-Si (MPS) structures in the frequency range of 10 – 200 KHz. *Journal of Elec Mater*, **46**: 4276-4286
- Bassler, H., Kohler, A., 2011. Synthesis of polypeptides by ROP of NCAs. *Peptide-Based Materials*, **310**: 1-26.
- Bera, S. C., Singh, R. V., Garg, V. K., 2008. Temperature behaviour and compensation of schottky barrier diode. *International Journal of Electronics*, **95**(5): 457-465.
- Bhattacharya, D. K., 2013a. *Solid State of Electronic Devices*. Solid state devices. 2013b.
- Brütting, W., 2006. *Physics of Organic Semiconductors*. Cardona, PeterY.Yu Manuel. Fundamentals of semiconductors.
- Cheung, S. K., Cheung, N. W., 1986. Extraction of schottky diode parameters from forward current-voltage characteristics. *Applied Physics Letters*, **49**(2): 85-87.
- Çaldıran, Z., Deniz, A. R., Aydoğan, S., Yesildag, A., Ekinci, D., 2013. Superlattices and microstructures the barrier height enhancement of the Au / n -Si / Al schottky barrier diode by electrochemically formed an organic anthracene layer on n -Si. *Superlattices and Microstructures*, **56**: 45-54.
- Demirezen, S., Sönmez, Z., Aydemir, U., Altındal, S., 2012. Effect of series resistance and interface states on the i-v, c-v and g/ω-v characteristics in au/bi-doped polyvinyl alcohol (pva)/n-si schottky barrier diodes at room temperature. *Current Applied Physics*, **12**(1): 266-272.
- Dongge, M., Yonghua, C., 2017. *Organic Semiconductor Heterojunctions and Its Application in Organic Light-Emitting Diodes*. Springer series in materials science 250.
- Ebisawa, F., Kurokawa, T., Nara, S., 1983. Electrical properties of polyacetylene/polysiloxane interface. *Journal of Applied Physics*, **54**(6): 3255-3259.
- Einspruch, N. G., Simon, S. C., 1988. *13 VLSI Electronics Microstructure Science*

- Metal-Semiconductor Contacts and Devices***. First edition. Academic Press.
- Fawen, G., 2014. **Low Noise High Detectivity Photodetectors Based On Organic Materials**. ETD collection for university of Nebraska - Lincoln: 1-138.
- Fereshteh, G., Amirmazlaghani, M., Raissi, F., 2012. Evaluation of photodetection properties of graphene-silicon schottky IR detector. ***International Journal of Green Nanotechnology: Biomedicine***, **4**(4): 464-469.
- Fetouhi, B., 2014. Junction characteristics system based on composite organic semiconductors : Polystyrene / polyaniline doped by [bmim] [bf 4] ionic liquid. ***Physical Chemistry***, **51**: 541-546.
- Gencer, I. A., 2016. Investigation of Al doping concentration effect on the structural and optical properties of the nanostructured cdo thin film. ***Superlattices and Microstructures***, **92**: 278-284.
- Gencer, I. A., Karaduman, O., Yakuphanoglu, F., 2016. Controlling of the photosensing properties of Al/dmy/p-si heterojunctions by the interface layer thickness. ***Synthetic Metals***, **221**: 114-19.
- Gencer, I. A., Ocak, Y. S., 2016. Effect of light intensity and temperature on the current voltage characteristics of Al/SY/p-Si organic–inorganic heterojunction. ***Journal of Electronic Materials***, **45**(10): 5347-5355.
- Gerhard, L., 2018. ***Semiconductor Radiation Detectors***. Springer Berlin Heidelberg New York
- Giyathaddin, O. M., 2015. ***Electrical and Photoelectrical Characterization of Au / ZrO 2 / n-Si mis*** (master thesis) T.R, Dicle university institute of natural and applied sciences, Diyarbakir.
- Hasan, H., Yildiz, D. E., 2019. Frequency dependent dielectric properties of ZnSe / p-Si diode. ***Politeknik Dergisi***, **22** (1): 63-67.
- Hyunsoo, K., 2015. Top illuminated organic photodetectors with dielectric / metal / dielectric transparent anode. ***Organic Electronics***, **20**: 103–11. <http://Dx.Doi.Org/10.1016/J.Orgel>.
- Kim, H., 2017. ***Organic Photodiodes and Their Optoelectronic Applications*** (Doctora thesis). The university of Michigan, Electrical and computer engineering. United States.
- Kohler, A., Bossler, H., 2015. ***Electronic Processes in Organic Semiconductors***. Wiley-VCH Verlag GmbH and Co. KGaA, Boschstr. 12, 69469 Weinheim, Germany.
- MOTT, N. F. 1939. The Theory of crystal rectifiers. ***Proceedings Of The Royal Society***, **171**(944): 27-38.
- Nalwa, H. S., 2001. ***Academi Press Supramolecular Photosensitive and Electroactive Materials***. Academic press.
- Norde, H., 1979. A modified forward I-V plot for schottky diodes with high series resistance. ***Journal of Applied Physics***, **50**(7): 5052-5053.
- Ocaya, R. O., 2016. Organic photodetector with coumarin-adjustable photocurrent. ***Synthetic Metals***, **213**: 65-72.
- Ostroverkhova, O., 2013. ***Handbook of Organic Materials for Optical and (Opto)Electronic Devices***. Woodhead publishing.
- Pearsall, P. T., 2013. ***Photonics Essentials***. McGraw-Hill Companies, Inc.
- Pierce, G. W., 1907. Crystal rectifiers for electric currents and electric oscillations. II. Carborundum, molybdenite, anatase, brookite. ***Proceedings Of The American Academy Of Arts and Sciences***, **44**(12): 317-349.

- Rudan, M., 2013. *Physics of Semiconductor Devices*. Springer science business media NewYork 2015.
- Sailor, M. J., Floyd, L. K., Robert, H. G., Nathan, S. L., 1990. Electronic properties of junctions between silicon and organic conducting polymers. *Nature*, **346**(6280): 155-157.
- Schlesinger, R., 2017. Energy-level control at hybrid inorganic/organic semiconductor interfaces. <http://link.springer.com/10.1007/978-3-319-46624-8>.
- Schottky, W., 1939. Halbleitertheorie der sperrschicht. *Die Naturwissenschaften*, **26**(52): 843-843.
- Schön, J. H., Ch, K., Bucher, E., Batlogg, B., 2004. Retraction note to: retraction: efficient organic photovoltaic diodes based on doped pentacene. *Nature*, **422**(6927): 93-93
- Sekhar, R. P. R., 2016. Modification of schottky barrier properties of Ti/p-type InP schottky diode by polyaniline (PANI) organic interlayer. *Journal of Semiconductor Technology and Science*, **16**(5): 664-674.
- Sze, S. M., Kwok, K. N., 2007. *Physics of Semiconductor Devices*. Third edition. John wiley and sons, jnc., publication.
- Tae, K. K., 2018. Studies on the fabrication and characteristics of organic photodiode using novel ga-doped NiOx as an electron-blocking layer. *Molecular Crystals and Liquid Crystals*, **662**(1): 91-95.
- Tahsin, K., Tombak, A., Ocak, Y. S., Aydemir, M., 2014. Electrical and photoelectrical characterization of a TTF/p-InP organic–inorganic heterojunction. *Microelectronic Engineering*, **129**: 91-95.
- Takehiko, M., 2016. *Electronic Properties of Organic Conductors Electronic Properties of Organic Conductors*. Springer, Japan.
- Tang, C. W., 1986. Two-layer organic photovoltaic cell. *Applied Physics Letters*, **48**(2): 183-185.
- Tascioglu, I., Aydemir, U., Altındal, S., Kınacı, B., Ozcelik, S., 2014. Analysis of the forward and reverse bias I-V characteristics on Au / PVA : Zn / n-Si Schottky barrier diodes in the wide temperature range. *Journal of Applied Physics*, **109**(5): 054502
- Tataroglu, A., 2018. Ruthenium(II) complex based photodiode for organic electronic applications. *Journal of Electronic Materials*, **47**(1): 828-833.
- Thomas, H. W., 2013. *Design and Fabrication Of Organic Semiconductor Photodiodes* (Doctor of Philosophy thesis). University of Florida, United States.
- Turut, A., Karabulut, A., Ejderha, K., Biyikli, N., 2015. Capacitance-conductance-current-voltage characteristics of atomic layer deposited Au/Ti/Al₂O₃/n-GaAs MIS structures. *Materials Science in Semiconductor Processing*, **39**: 400-407.
- Ventalon, V., 2016. Organic photodiode for detection of herbicides in water using microalgal photosynthesis. *Nanotechnology Materials and Devices Conference, NMDC 2016 - Conference Proceedings*.
- Williams, R. H., 1983. *Semiconductor Surfaces and Interfaces*. Springer-Verlag Berlin Heidelberg.
- Winfried, M., 1994. Metal-semiconductor contacts: electronic properties. *Surface Science*, **6028**(1): 928-944.
- Yaşar, S., 2018. Electrical and photoelectrical characterization of organic-inorganic heterostructures based on ru-n-heterocyclic carbene complexes. *Optik*, **156**: 514-

521.

Yuan, L., 2018. Approaching the schottky-mott limit in waals metal – semiconductor junctions. *Nature*. <http://dx.doi.org/10.1038/s41586-018-0129-8>.



**EXTENDED TURKISH SUMMARY
(GENİŞLETİLMİŞ TÜRKÇE ÖZET)**

**OPTOELEKTRONİK UYGULAMALAR İÇİN ORGANİK BİLEŞENLİ
FOTODİYOTUN ÜRETİMİ VE PARAMETRELERİNİN BELİRLENMESİ**

MAHMOOD, Othman Haji
Yüksek Lisans Tezi, Fizik Anabilim Dalı
Tez Danışmanı: Doç. Dr. Arife GENÇER İMER

ÖZ

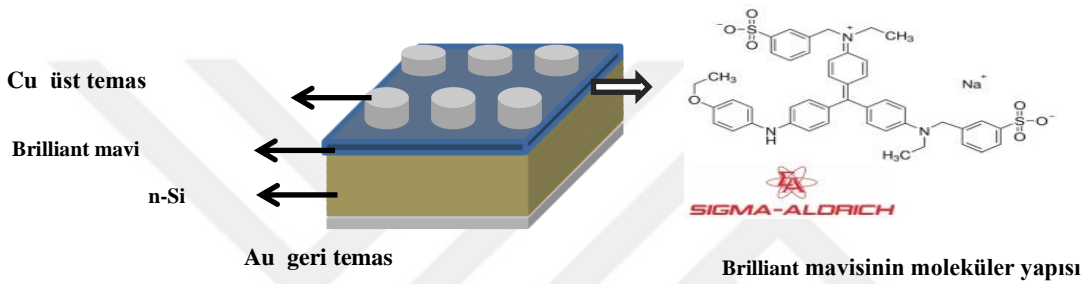
Bu tez çalışmasında, parlak mavi (BB) bileşenli heteroeklem aygıtların elektronik ve optoelektronik parametreleri belirlenmiştir. Çalışmada, (100) yönelimine sahip ve öz direnci 1-10 Ω -cm olan n-Si yarıiletken kristali üzerine, metanolde çözülerek hazırlanmış 1×10^{-2} molarlık organik boyar çözelti dönel kaplama (spin coating) metoduyla ince organik arayüzey tabaka olarak kaplanıp, yüksek vakum ortamında bakır metali (Cu) termal buharlaştırılarak Cu/BB/n-Si/Au hibrit yapıları elde edilmiştir. Üretilen aygıtların elektriksel ve fotoelektriksel karakteristik özellikleri incelenip analiz edilmiştir.

Aygıtların elektriksel parametreleri oda sıcaklığında ve karanlık ortamda akım-gerilim (I - V) ve kapasite-gerilim (C - V) ölçümleri yardımıyla incelendi. Buna göre her aygıtta düz beslem I - V ölçümlerinden idealite faktörü, engel yüksekliği gibi elektrik parametreleri Cheung, Norde fonksiyonları yardımıyla hesaplanmıştır. Tüm yöntemlerden elde edilen sonuçların mukayesesi yapılarak tartışıldı. Elde edilen tüm bulgulara dayanarak elektriksel ve fotoelektriksel parametrelerin organik film yardımıyla iyileştiği tespit edilmiştir.

Anahtar kelimeler: Engel Yüksekliği, Foto diyot, Organik arayüzey.

1. MATERYAL VE YÖNTEM

Tez çalışmasında; parlak mavi molekülü organik arayüzey olarak kullanılarak organik/inorganik yarıiletken heteroeklem aygıtlar üretilmiştir. Şekil 1 de MIS kontak yapının şematik gösterimi verilmiştir. Üretilen kontakların akım-gerilim ve frekans bağımlı kapasitans gerilim ölçümleri oda sıcaklığına karanlıkta ve farklı aydınlanmalar altında yapılmıştır.



Şekil 2.1. Metal/Organik molekül/n-Si yapısının şematik gösterimi.

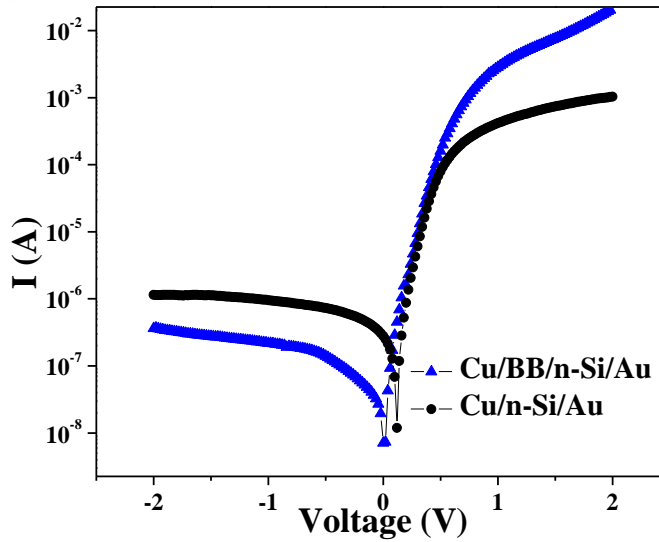
Aygıtın akım-voltaj ölçümlerinden elde edilen grafiklerden, hetero yapının doğrultucu özelliği incelendi ve engel yüksekliği ve idealite faktörü gibi önemli elektriksel parametreleri belirlendi. Ek olarak Cheung ve Norde fonksiyonları kullanılarak bu iki değer yeniden hesaplanıp sonuçların doğruluğu kontrol edildi ve diyotun seri direnci hesaplanmıştır.

İkinci aşamada optoelektronik uygulamalar açısından değerlendirebilmek için, akım-gerilim ölçümleri farklı ışık şiddetleri altında alındı. Bu ölçümler yardımıyla, ışık duyarlılığı, ışık algılaması, ışık tepkisi, lineer dinamik aralığı gibi fotodiyot parametreleri belirlenmiştir.

Foto akımının karanlık akıma oranı ışık duyarlılığı olarak tanımlanır. Yine Lineer dinamik aralık (LDR) önemli bir özelliktir ve fotodiyotlar için önemli belirleyici bir değeridir. Fotodiyotun ışık duyarlılığı özelliğinin nicel analizi, fotoakımın aydınlanma gücüne olan bağımlılığı incelenerek belirlenebilir. Fotodiyotun, gelen ışık şiddetinin bir fonksiyonu olduğu saptanmıştır.

2. BULGULAR VE TARTIŞMA

Bu tez kapsamında sunulan çalışmada, daha önce kullanılmamış bir organik boyar madde yardımıyla, Au/n-Si heteroeklemin performansının değişimi incelenmiştir. Şekil 3.1 karanlık ortamda oda sıcaklığında yapılan akım-voltaj ölçümlerinin grafikleridir. Bu grafikte ters beslem akımının zayıf bir voltaj bağımlılığı gösterdiği, doğru beslem akımının ise gerilim ile eksponansiyel olarak arttığı görülmektedir. Arayüzey içeren ve içermeyen her iki örnek de doğrultucu özellik göstermiştir. Doğrultma oranı arayüzey içeren örnekte daha yüksektir. İdealite faktörü (n) ve engel yüksekliği (Φ_b) Ag/n-Si ve Ag/BB/n-Si örnek için sırasıyla 1.50, 1.36 ve 0.74, 0.83 eV olarak hesaplanmıştır. Heteroeklem arayüzeylerinden kaynaklanan ideal olmayan davranışlar gösterir. Sonuç olarak, elde edilen sonuçlar bariyer yüksekliğinin BB organik boyar maddenin ince film arayüzey tabakası tarafından değiştirilebilirliğini, ve modifikasyonun olabilirliğini ortaya koymuştur.

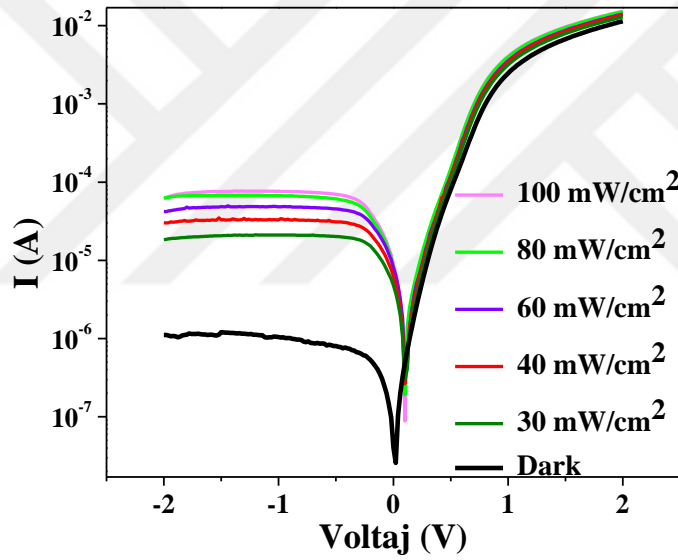


Şekil 3.1. Ag/n-Si ve Ag/BB/n-Si aygıtlarının yarılogaritmik I-V grafikleri.

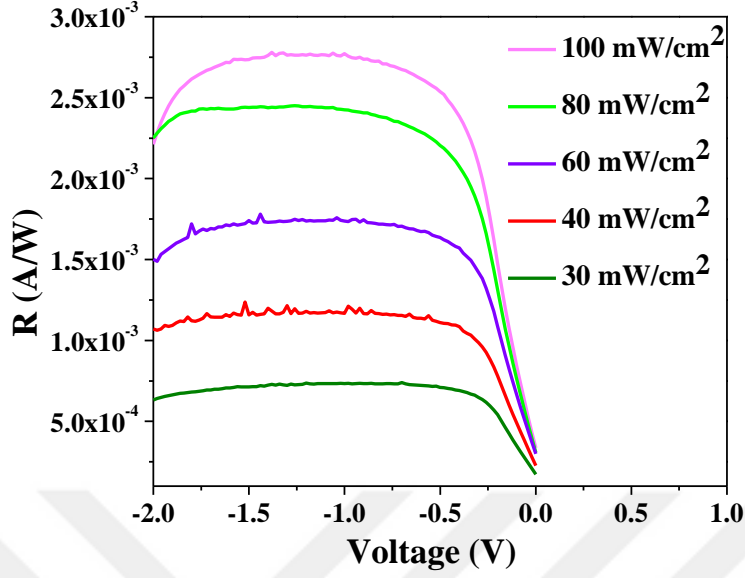
Şekil 3.2. ışığın çeşitli aydınlatma yoğunlukları altındaki heteroeklem aygıtın I-V karakteristiği üzerindeki etkisini göstermektedir. Şekilde, aydınlanma şiddeti arttıkça

ters beslem foto akımının arttığı görülmektedir. Bu durum foto akımın gelen ışığın enerjisinin soğurulması sayesinde taşıyıcı üretimi yoluyla oluştuğu anlamına gelir. Bununla birlikte farklı aydınlatmalar altında I - V ölçümleri alınmış, cihazın ışığa duyarlılık özelliklerini anlamak için bazı fotoelektriksel parametreleri hesaplanmıştır. Aygıtın optik sensör veya fotodiyot gibi optoelektronik uygulamalarda kullanılabileceği doğrulanmıştır.

Şekil 3.3. cihazın ışık algısının gerilimin fonksiyonu olarak değişimini gösterir. Işık responsu 0.3 V değerinden sonra stabil kabul edilebilir. En büyük ışık duyarlılığı en yüksek ışık şiddeti olan 100 mW/cm^2 aydınlanma şartında $2.75 \times 10^{-3} \text{ A/mW}$ olarak elde edilmiştir.



Şekil 3.2. Ag/BB/n-Si heteroeklemin farklı ışık şiddeti altında $\ln(I)$ - V grafikleri.



Şekil 3.3. Ag/BB/n-Si heteroeklemin farklı ışık şiddeti altında R-V grafikleri

Bu araştırmanın özgün değeri ve bilimsel açıdan önemi aşağıdaki şekilde vurgulanabilir:

(i) Bu çalışmada incelenmesi hedeflenen organik arayüzey kullanılarak doğrultucu kontak üretilebilirliği, ve kontak karakteristiklerinin organik materyal yardımıyla modifiye edilebilirliği, yarı iletken aygıt üretimi açısından çok büyük öneme sahiptir. Bununla beraber, birden fazla sayıda sistematik olarak üretilip, incelenecek olan organik/inorganik yarıiletken eklemlerin akım-voltaj ölçümleri beklentiler doğrultusunda sonuçlanmış ve optoelektronik aygıt üretimine elverişliliği rapor edilmiştir.

(ii) Bu çalışmanın birincil önemi seçilen organik boyar maddenin elektronik aygıt performansını iyileştirmesine ilişkindir. Organik boya maddesinin (brilliant mavisi) Schottky tipi kontaklarda arayüzey elemanı materyali olarak kullanıp, bu kontakların doğrultucu ya da omik özelliklerini incelemesi ve akım-voltaj (I-V) ve kapasitans-voltaj/frekans (C-V/C-F) ölçümleri ve grafikler yardımıyla doğrultucu özellik gösterdiği ortaya koyulmuştur. Daha önce arayüzey elemanı olarak kullanılmamış olan bu organik boyar madde ile elektronik özelliklerin iyileştiği organik arayüzey içermeyen referans aygıt ile karşılaştırmalı olarak gösterilmiştir.

(iii) Bu çalışmanın ikincil önemi seçilen organik molekül ile doğrultucu elde edildikten sonra, farklı aydınlanmalar altında üretilen aygıtların ışık duyarlılığına ve fotodiyot özelliklerine ilişkindir. Elde edilen bulgular yardımıyla, organik arayüzey filmin fotodiyot parametrelerine etkileri deneysel olarak ortaya konmuştur. Ayrıca ışık algısı beklenen ölçüde olduğu belirlendiğinden, üretilen aygıtın farklı optoelektronik uygulamalar için iyi bir aday olduğu rapor edilmiştir.

3. SONUÇ

Parlak mavi boyar maddesinin bir elektronik aygıtın metal yarıiletken arayüzeyinde ilk defa kullanılması tezin temel özgünlüğünü oluşturmaktadır. Bu çalışmada elde edilen bulgular parlak mavi organik boyar maddesinin üretilen heteroeklemin elektriksel parametrelerini iyileştirdiğini ve bu parametrelerin organik arayüzey ile modifiye edilebilirliğini göstermiştir. Ayrıca, ışık altında yapılan ölçümler sayesinde aygıtın düşük beslem değerlerinde duyarlılığa sahip olduğu görülmüştür. Ek olarak, aygıtın ışık duyarlılığını ve optoelektronik uygulamalarının olasılığını araştırmak için yapılan analizlerde, kullanılan aygıtın yeterince ışık duyarlılığına sahip olduğu ve optoelektronik teknolojisinde fotodiyot yapımında kullanılabileceği rapor edilmiştir.

CURRICULUM VITAE

Personal Information

Othman Haji Mahmood

Date of birth and place: 10/01/1990 – Sulaymaniyah

Home address: Iraq / Erbil-Kasnazan

Tel: (+90) 538 864 35 46 – (+964) 750 425 25 53

Email: Othmanhaji1990@gmail.com

Education and Study

09/2005 – 07/2009 Graduated from Shahid Dr.abdulrahman Preparatory School for boys.

09/2009 – 07/2013 Graduated from Salahaddin Univerty – Erbil / College of Education/ Physics department with ranking 1st among fifty students.

02/2018 Continues study M.Sc with thesis – Solid state physics in Van Yuzuncu Yil university – institute of natural and applied Science – Physics Department.

Job Experience

09/ 2013 up to now Assist Physicist at Salahaddin University/Hawler College of Education/ Scientific Department. Dept. of Physics.

06/2014 – 11/2014 Privet lecturer at Bahez Institue of Progress Skills – Erbil.

11/2014 – 03/2015 lecturer at Hasarok basic schools.

03/2015 – 06/2015 lecturer at Shabange evening preparatory school for girls.

Language Skills

Native language Kurdish

Foreigner language English (good), Arabic (moderate), Turkish (weak)

Computer Skills

Microsoft office (Word- Excel - Powerpoint)

Matlab

Mattcad

Photoshop

Origin Pro8

Grapher

Academic Activity

PCFM Conference – Elazig on July, 2018 with two poster presentations under the title of:

Ugur.A, Gencer Imer.A, Mahmood.O, Omarbly.S, Ocak.Y., 2018. The Electrical Parameters Of *Al/Tb/P-Si* Heterojunction Device. *Physical Chemistry and Functional Materials*. 67-67 july 2018, Elazig.

Ugur.A, Gencer Imer.A, Mahmood.O, Omarbly.S, Ocak.Y., 2018. The Graphene Oxide Doped ZnO Nanostructured Films Prepared by Ultrasonic Spray Prolysis. *Physical Chemistry and Functional Materials*. 17-17 july 2018, Elazig.

ICSMD Conference - Ardahan on September, 2018 two presentations under the title of : Mahmood.O, Gencer Imer.A, Ocak.Y, Tombak.A., The Photocatalytic Degredation of Methylen Blue Dye By Pure And Tin Doped Cadmium Oxide Nanostructured Film. **2nd International Congress on Semiconductor materials and Devices**. 42-46 September 2018, Ardahan.

Mahmood.O, Gencer Imer.O, Korkut.A., The Comparative Study on The Electrical Parameters of Ag/N-Si And Hybrid Structure Based on Organic Interlayer. **2nd International Congress on Semiconductor materials and Devices**. 42-46 September 2018, Ardahan.